Differentiation and Maturation Effect of All-trans Retinoic Acid on Cultured Fetal RPE and Stem Cell-Derived RPE Cells for Cell-Based Therapy

Tingyu Yan
Fourth Affiliated Hospital of China Medical University
Na Yang
China Medical University
Wei Hu
Affiliated Hospital of Weifang Medical University
Xinxin Zhang
Fourth Affiliated Hospital of China Medical University
Xuedong Li
Fourth Affiliated Hospital of China Medical University
Youjin Wang
Fourth Affiliated Hospital of China Medical University
Jun Kong (kongjun@hotmail.com)
Fourth Affiliated Hospital of China Medical University https://orcid.org/0000-0002-7880-2578

Research

Keywords: retinal pigment epithelium, human embryonic stem cells, human induced pluripotent stem cells, epithelial-mesenchymal transition, all-trans retinoic acid, cell-based therapy

Posted Date: December 16th, 2020

DOI: https://doi.org/10.21203/rs.3.rs-127315/v1

Abstract

Background: Phase I/II clinical trials using fetal retinal pigment epithelium (fRPE), human embryonic stem cell (hESC)-derived RPE, or human induced pluripotent stem cell (hiPSC)-derived RPE as potential sources of materials for cell-based therapy to treat degenerative retinal diseases have been carried out during the past decade. Challenges for successful translational cell-based therapy include cell manufacture, cell quality, cell storage, and cell behavior in vivo. In this study, we investigated the culture-induced changes in passaged fetal RPE, hESC-RPE and hiPSC-RPE cells in vitro and explored the differentiation and maturation effect of all-trans retinoic acid (ATRA) on those RPE cells.

Methods: A total of 9 fetal RPE cell lines, hESC-RPE and hiPSC-RPE cell lines were set up using previously described methods. The culture-induced changes in subsequent passages caused by manipulating plating density, dissociation method and repeated passaging were studied by microscope, real-time quantitative PCR, western blot and immunofluorescent assays. Gene and protein expression and functional characteristics of fRPE, hESC-RPE and hiPSC-RPE incubated with ATRA at different concentration were also evaluated.

Results: Compared with fRPE, hESC-RPE and hiPSC-RPE showed decreased gene and protein expression of RPE markers. P3 RPE of all three types seeded at a density of 6×10^5 and 9×10^5 cells/mL in basal medium maintained pigmented polygonal, cobblestone-like morphology. RPE cells underwent mesenchymal changes showing increased expression of mesenchymal markers including a-SMA, N-cadherin, fibronectin and decreased expression of RPE markers including RPE65, E-cadherin and ZO-1, as a subsequence of low plating density, inappropriate dissociated method, and repeated passaging. fRPE, hESC-RPE and iPSC-RPE treated by ATRA at different concentrations showed increased expression of RPE markers such as RPE65, bestrophin (BEST) and CRALBP, and increased expression of negative complement regulatory proteins (CRP) including complement factor H (CFH), CD46, CD55 and CD59, and increased transepithelial resistance (TER) as well.

Conclusion: Although hESC and hiPSC-derived RPE are morphologically similar to fRPE, and also have the tendency to undergo epithelial-to-mesenchymal transition (EMT) changes during the culturing and passaging process in *vitro,* differences in protein and gene expression among three RPE types exist. Moreover, ATRA can increase RPE markers expression, as well as to increase the expression levels of CRPs gene and protein in fRPE and stem cell-derived RPE.

Background

Age-related macular degeneration (AMD) is a chronic degenerative disease that is the leading cause of social blindness in populations over the age of 50 [1]. The advanced stages of AMD are characterized by atrophic (dry) and/or neovascular (wet) forms. Anti-vascular endothelial growth factor (VEGF) treatments are effective in avoiding substantial visual acuity loss from neovascular AMD [2, 3]. However, there is as yet no effective treatment for dry AMD [4]. Stargardt disease, the most common retinal dystrophy in

children with a prevalence of 1:10,000 births [5], caused by monogenetic defects, has several similarities to dry AMD. The impaired and complete loss of retinal pigment epithelium (RPE) cells is the main cause of irreversible blindness in dry AMD and Stargardt disease [6]. Because RPE cells are mainly non-proliferative throughout life, a variety of cellular regenerative therapies with different cell types including human embryonic stem cell (hESC)-derived RPE [7, 8] and human induced pluripotent stem cell (hiPSCs)-derived RPE [9–11] as well as primary RPE cells from fetal tissues [12] are being studied as a potential treatment of advanced AMD and Stargardt disease [13].

Clinical trials of cell transplantation of fRPE, hESC-RPE and hiPSC-RPE for retinal degenerative disease are currently in progress. Great challenges in clinical application of cell-based therapy include lack of gold standards in cell manufacture, cell identification, cell quality assessment, cell purity and cell behavior *in vivo*. Better methods for producing and expanding large amounts of high quality RPE are still undertesting. Ways of delivering cells into subretinal space include cell suspension injection or cell sheet transplantation. For successful cell replacement, donor cells must survive, integrate, and function physiologically *in situ*. The subretinal microenvironment can affect cell survival and functionality of the transplanted cells. Thus, it is hypothesized that transplantation of differentiated and mature RPE donor cells may increase survival rate *in vivo* and maintain proper functions in the areas of atrophy [14–16]. In *vitro* cultured RPE that have cobblestone-like morphology, express RPE markers and have phagocytic functions, are considered as differentiated RPE cells. However, it's not sure whether they can play complex roles as those of the natural RPE, such as secretion growth factors, transportation of metabolites, reducing photo-oxidative stress and mediation of the immune response. Moreover, it has been well known that cultured human adult RPE cells may exhibit considerable phenotypic variation depending on their growth conditions [17], such as cell seeding density, culture medium, or passage number [18]. The most common problem is that passaged human adult RPE cells have tendencies to undergo epithelial-to-mesenchymal transition (EMT), losing the cobblestoned morphology and pigmentation [19]. However, very few investigations have studied the EMT changes in cultured fetal RPE and stem cell-derived RPE cells, which may compromise the outcome of cell-based therapy for degenerative diseases. Dr. Singh. R. *et al* tested the effects of serial expansion on hiPSC-derived RPE cultures and demonstrated that Passage (P) 4 hiPSC-RPE failed to proliferate and reform monolayers and showed significant decrease in the expression of key RPE marker genes but increase in the expression of mesenchymal markers [20]. All these questions mentioned above arose the concerns that standard manufacture protocols should be bring up to decrease discrepancy from cell batch to batch, to avoid the EMT changes in the donor RPE cells and to maintain high standards of cell quality.

Retinoic acid, a derivative of vitamin A and biologically active metabolite of visual transduction pathway, regulates cell growth, differentiation, and matrix formation in various types of tissues and is necessary for both normal and diseased eye [21]. All-trans retinoic acid (ATRA) can up-regulate the expression of tight junction-associated protein in the retinal pigment epithelium (RPE)-choroid complex, and promotes the epithelial barrier function of the RPE monolayer during the development of myopia [22–24]. Studies also showed that ATRA can inhibit immortalization of human epidermal keratinocytes during or after

transfection with human papilloma virus (HPV) 16 [25]. The most remarkable example of the role of ARTA as differentiating agents is the complete remission in patients with acute promyelocytic leukaemia in oncology practice. Based on these results and the fact that ARTA plays important role in the differentiation and development of the normal retina, we hypothesized that adding ARTA into fRPE and stem cell-derived RPE culture medium may help further differentiation of the passaged RPE and promote their physical behaviors. In this study, we studied the factors that may influence pigmentation, morphology and gene expression of passaged fetal RPE, hESC-derived and hiPSC-derived RPE, and investigated if ATRA could promote differentiation and maturation of fetal RPE and stem cell-derived RPE.

Matherials And Methods

Cell culture

The protocol of this experiment was approved by Ethical Review Committee of China Medical University. Fetal tissue was gained with informed consent following elective termination of pregnancy at 15–22 weeks of gestation. Human skin tissues were collected from healthy donors who were well consented and signed the informed consent.

Dissociation and Expansion of Fetal RPE

Three fetal RPE (fRPE) cell lines were generated for this study. Fetal eyes were acquired from abortion donors in the First Hospital of China Medical University. fRPE was isolated and cultured as the methods described by Arvydas Maminisbkis *et al* [26] and Ilene K. Sugino *et al* [12]. fRPE layer were mechanically separated from the choroid and cultured in MEM (Sigma-Aldrich) supplemented with 10% heat inactivated fatal bovine serum (FBS, Gibico), 2 mM L-glutamine (Gibico)、100 U/mL Non-essential amino acids (NEAA, Gibico)、1% Penicillin-Streptomycin (Gibico), 1% N1 supplement (Insulin, Transferin and Sodium selenite; Sigma), THT (250 mg/LTaurine、0.013 ug/L Triiodo-thyronin and 20 ug/L Hydrocortisone; Sigma) at 37 ℃ in 5% CO2. These cells were termed Passage 0. After 1 week, the medium was changed to 5% serum-containing RPE medium (DMEM (high glucose) with 7% knockout serum replacement, 2 mM GlutaMAX, 0.1 mM MEM NEAA, 0.1 mM β-mercaptoethanol (Invitrogen), 5% FBS, and 10 ng/mL basic fibroblast growth factor (bFGF) being included until cells reached confluence. The RPE medium was changed every 2–3 days.

First, passage 2 fRPE which had been cultured for more than a month were dissociated by 0.25% trypsin for 30 to 40 minutes and plated at densities of 9×10^5 cells/mL, 6×10^5 cells/mL, 3×10^5 cells/mL and 1×10^5 cells/mL respectively on 0.1% gelatin-coated 6-well plates (Corning) to test the effect of plating density on EMT changes.

Second, passage 2 fRPE which had been cultured for more than a month were dissociated by 0.25% trypsin for up to 20 minutes or at least 30 minutes respectively to test the effect of dissociating method

on EMT changes. The residual attached RPE cells were scraped, washed and mixed to the cell suspension.

Third, passage 2 fRPE which had been cultured for more than a month were serially passaged to passage 6 with a plating density of 6×10^5 cells/mL to test the effect of passaging number on RPE morphology and gene expression.

Differentiation and maintenance of hESC-RPE

The hESC lines were gifts from Dr. Weidong Li (Bio-X institutes at Shanghai Jiao Tong University). Three hESC lines were included in this study. We followed the hESCs culture method described by Ilene K. Sugino *et al* [12]. hESCs were cultured in six-well cell culture plates coated with 0.1% gelatin and seeded with CF-1 mouse embryonic fibroblast (MEF) feeders. Cells were maintained in Dulbecco's Modified Eagle Medium Nutrient Mixture F-12 (DMEM/F12, Gibco) with 20% Knockout Serum Replacement (Invitrogen), 1% non-essential amino acid solution, 1% GlutaMAX, 10 ng/mL bFGF (Invitrogen) and 0.1 mM β-mercaptoethanol. For RPE induction, the protocol of differentiation of hESCs to RPE was adapted from Buchholz et al [27]. Stem cells were switched to bFGF-free hESC medium when hESC colonies were confluent. Pigmented foci arose from differentiating hESCs after 3–4 weeks of exposure to bFGF-free hESC medium. Once the pigmented clusters reached about 1 mm in diameter, they were manually excised by syringe needles under a dissecting microscope and seeded in gelatin-coated 6-well plates. hESC-RPE were allowed to expand for a further 1–2 months in the RPE medium. These cells were defined as primary culture, passage (P) 0, and were evaluated and passaged every 1–2 months as described above.

Reprogramming of human fibroblasts and RPE differentiation

Three hiPSC lines were generated from three healthy donors' skin fibroblasts. Episomal iPSC Reprogramming Vectors containing Oct3/4, Sox2, Klf4, and c-Myc were used for reprogramming fibroblasts into induced pluripotent stem cells (iPSCs). Selected colonies were picked and passaged to establish individual iPSC lines, which were subsequently maintained in culture under feeder-free conditions, using a 1:1 formulation of TeSR2 medium (05860; Stem Cell Technologies) and NutriStem® medium (01–0005; Stemgent). The pluripotency of hiPSC was also confirmed with immunofluorescent histochemistry and teratoma formation assays. hiPSC were differentiated into RPE by following the protocol described above as for differentiating hESC-RPE. Passage 3 was used for the further study.

All-trans retinoic acid preparation and cell treatment

A 10 mM stock solution was prepared in ethanol and stored at − 20 ℃ in the dark and diluted with cell culture medium right before use. P3 fRPE, hESC-RPE and hiPSC-RPE were seeded and cultured for approximately 4 weeks to reach confluence, then, cells were incubated with RA at concentrations ranging from 10^{-8}, 10^{-7} to 10^{-6} M for another 2 hours or 24 hours respectively for RNA test, 1 week for Western Blot test, and 2 weeks for transepithelial resistance assay. During the incubation period, the cultured medium was replaced every other days with fresh prepared RA.

RNA isolation and real-time RT-PCR (RT-qPCR)

Total RNA was extracted using TRIzol reagent (TaKaRa) and cDNA was synthesized with a reverse transcription kit (TaKaRa) according to the manufacturer's instructions. qRT-PCR was carried out using SYBR PrimeScript RT-PCR kit (TaKaRa) in a 384 well format on a 7500 Sequence Detection System (Applied Biosystems, Foster City, CA). Gene expression levels were quantified using the $2^{-\triangle\triangle Ct}$ method of relative quantification(RQ)and the transcript levels were normalized relative to the B-actin or GAPDH mRNA or 18sRNA in each sample. The primers sequences were listed in Additional file 1: Table S1.

Western blot analysis

After being washed twice with cold phosphate-buffered saline (PBS), confluent cultured cells were detached using a cell scraper and lysed in 100 ul cold RIPA buffer supplemented with phenylmethylsulfonyl fluoride (PMSF; a protease inhibitor). The cell lysates were collected after centrifugation at 13,000 rpm for 10 min and the protein concentration was determined by bicinchoninic acid method (BCA, Beyotime). The protein samples were separated by SDS-polyacrylamide gel electrophoresis and transferred into polyvinylidene difluoride membranes (PVDF, Millipore). The membranes were blocked with 5% non-fat milk for 1 hour at room temperature, followed by incubation with antibodies directed against RPE65 (Abcam), E-cadherin (Proteintech), ZO-1 (Invitrogen), α-SMA (Proteintech), FN (Abcam), N-cadherin (Proteintech), GAPDH (d 1:1000 in Tris-buffered saline containing 0.1% Tween-20 (TBST). PVDF membranes were washed three times in TBST and incubated for 2 hours with secondary antibody at room temperature. The protein was visualized using enhanced chemiluminescence (ECL).

Immunofluorescence

Cells were fixed in 4% paraformaldehyde in PBS for 20 minutes at room temperature and treated with 0.2% Triton X-100 for 15 minutes on ice. Cells were further blocked with 5% bovine serum albumin (BSA) in PBS for 1 hours at room temperature. Controls were included in each determination by the omission of primary and secondary antibodies. The cell samples were incubated with the primary antibody (CRALBP, ZO-1, bestrophin, RPE 65, E-cadherin, N-cadherin, FN, α-SMA) overnight at 4 °C and incubated with secondary antibody (goat anti-mouse Alexa Fluor 488 dilution (1:200, color green) and goat anti-rabbit Alexa Fluor 546 dilution (1:200, color red) for 1 hours at room temperature. Nuclear were stained with DAPI blue. Images were acquired using Inverted Fluorescence Microscope.

Measurement of transepithelial resistance (TER)

To evaluate the barrier function of these three types of RPE cells cultured with or without ATRA, TER measurements were performed on the 9 RPE cell lines (3 for each RPE type) respectively. P3 fRPE, hESC-RPE and hiPSC-RPE which were cultured for more than one month were incubated with RPE medium containing 10^{-7} M of ATRA for two more weeks, while the control groups were cultured in RPE medium without ATRA. Culturing medium was changed every other day. Two weeks after ATRA treatment, TERs of

the RPE cell monolayers were measured using a Millicell ERS-2 Voltmeter (Merch Millipore). TERs of different groups were calculated as the average of three measurements.

Statistical Analysis

Data were presented by the means ± standard deviation of the mean. A two-tailed Student *t* test was used to determent whether there was a significant difference between two groups. Significance was reported for *P* values less than 0.05.

Results

Generating and Identification of hiPSCs

Fibroblast cells started to migrate and expand from skin tissues at 2–7 days after plating (see Additional file 2: Fig. S1A). Fibroblast cells at passage 3 were cotransfected by the four reprogramming vectors and primarily cultured in fibroblast medium followed by iPSC medium (see Additional file 2: Fig. S1B). Colonies started to emerge at week 2. At day 30, tightly packed dome-like colonies were picked up and replated onto mouse embryonic fibroblasts (MEFs), noted as passage 0 (P0) (see Additional file 2: Fig. S1C). Expanded hiPSC colonies (see Additional file 2: Fig. S1D) developed alkaline phosphatase (AP) activity along with expression of the pluripotency markers OCT4, Sox-2, SSEA4 and TR-1-60, confirmed by immunofluorescence staining (see Additional file 2: Fig. S1E-G).

Morphological phenotypes and RPE-specific gene expression in fRPE, hESC-RPE and hiPSC-RPE cultured in vitro

Primary fetal RPE cultured for 1 month formed pigmented epithelial monolayer and exhibited heavy pigmentation with cobblestone-shaped morphology and tight junctions in a regular hexagonal mosaic (see Additional file 3: Fig. S2A).

hESC lines were split every five days. Pigmented clusters spontaneously arose from differentiating hESCs after being cultured 2 to 4 weeks in bFGF-free hESC culture media (see Additional file 4: Fig. S3A). RPE-like cells showed up after pigmented clusters were manually dissected and expended in 24-well plate (see Additional file 4: Fig. S3B-C). hESC-RPE exhibited typical morphology and structural characteristics of RPE (see Additional file 3: Fig. S2B). Similar to hESC-RPE differentiation, 2 to 4 weeks after withdraw bFGF from hiPSC culture medium, pigmented cluster spontaneously arose and cells with cobble-stoned morphology formed. Pigmented clusters were manually dissected and plated to gelatin-coated plates and cultured with RPE medium, defined as P0.

After being cultured for 2 to 3 months, RPE cells from different sources showed robust expression of RPE signature proteins, including RPE65, bestrophin and ZO-1 by immunocytochemistry (Fig. 1). However, the expressions of RPE related markers were more robust in fRPE cells than those of stem cells derived RPE

cells. hiPSC-RPE cells showed weakest expression of the RPE related markers among the three types of RPE cells.

Effects of cell plating density, passage numbers and dissociating methods on the morphology of passaged fRPE, hESC-RPE and hiPSC-RPE cells

RPE cells were passaged at different densities. Cell morphology at 24 hours and 1 month of culturing are shown in Fig. 2. Results revealed that P3 cells passaged at a density of 9×10^5 cells/mL and 6×10^5 cells/mL expanded sheets and exhibited polygonal, cobblestone-like morphology after 24 hours of culture, while fRPE cells passaged at lower densities of 1×10^5 cells/mL and 3×10^5 cells/mL exhibited a fibroblast-like morphology with increased size (Fig. 2A). After being cultured in vitro for 1 month, P3 cells plated at a higher density were morphologically similar to P1 cells except showing less pigmentation. P3 cells plated at a density of 3×10^5 cells/mL exhibited epithelial morphology in the center of the culture plates, whereas cells in the peripheral area showed fusiform and disorganized shapes. P3 cells plated at lowest density showed remarkable characteristics of mesenchymal cells.

Next, the cell morphology in different passage numbers was compared. fRPE which had been cultured for more than a month were serially passaged to passage 6 with a plating density of 6×10^5 cells/mL to test the effect of passaging numbers on RPE morphology and gene expression. The fRPE cells could maintain typical RPE morphology and heavy pigmentation over four passages (P0-P3). However, cells in passage 4 and passage 5 showed less pigmentation and cells in the peripheral areas of the P5 culturing plate started to exhibit a fibroblast-like morphology. Moreover, cells in passage 6 had abundant mesenchymal characteristics (Fig. 2B). P3 cells and P5 cells were processed for Hematoxylin-Eosin (HE) Staining after being cultured for 24 hours. HE-staining results showed that P3 cells exhibited polygonal, cobblestone-like morphology with melanosome granules around the nuclear, while the P5 cells showed spindle shape with less pigmentation (Fig. 2C).

In addition, to observe the effect of dissociating method on cell morphology, P3 fRPE plated at 6×10^5 cells/mL were cultured for 1 month. The P3 cells dissociated by 0.25% trypsin for 30 to 40 minutes maintained polygonal, cobblestone-like morphology and heavy pigmentation, while, the cells dissociated by 0.25% trypsin for less than 20 minutes started to exhibit fibroblast-like morphology (Fig. 2D). hESC-RPE and hiPSC-RPE cells showed similar trends (see Additional file 5: Fig. S4).

Expression of RPE markers and mesenchymal markers in fRPE and stem cells derived RPE cells

P1 and P5 fRPE cultured for 1 month were compared. Using RT-qPCR analysis, we assayed the mRNA expression levels of RPE markers including RPE65, ZO-1, E-cadherin and mesenchymal markers including α-SMA, FN, N-cadherin. We found that expression of RPE65, E-cadherin and ZO-1 in fRPE cells that

underwent EMT changes were significantly decreased and expression of a-SMA, N-cadherin and FN were significantly increased by 4.12 folds, 3.21 folds and 10.26 folds, respectively ($P < 0.05$) (Fig. 3A). In a parallel approach, western blotting results demonstrated that protein expression of RPE markers was downregulated and the protein expression of EMT markers was upregulated in EMT-fRPE cells. (Fig. 3B). In addition, immunocytochemistry results strengthened the findings (Fig. 3C-D).

hESC-RPE cells undergoing EMT showed similar trends in most of gene expression. Interestingly, EMT hESC-RPE cells showed comparable gene expression levels to EMT fRPE in most of the genes we observed except E-cadherin. E-cadherin expression was not downregulated in EMT hESC-RPE cells (Fig. 4).

hESC-RPE RPE cells express RPE markers

Further, we determined whether the expression levels of RPE-marker genes in hESC-RPE were comparable to those of fRPE (Fig. S5). We found that the mRNA expression levels of RPE-related markers in hESC-RPE cells (P1, Day 28) were significantly lower than those of fRPE cells in general (P1, Day 28).

Effect of ATRA on expression of RPE-specific genes and complement negative regulatory proteins (CRPs) in fRPE, hESC-RPE and hiPSC-RPE cells

P3 fRPE, hESC-RPE and hiPSC-RPE were seeded and cultured for approximately 4 weeks to reach confluence, then, cells were incubated with RA at concentrations ranging from 10^{-8}, 10^{-7} to 10^{-6} M for another 2 hours or 24 hours respectively for RNA test, 1 week for Western Blot test, and 2 weeks for transepithelial resistance assay. As shown in Fig. 5, in the fRPE group, 2-hour incubation with ATRA in concentrations of 10^{-6} ,10^{-7} and 10^{-8} M resulted in an increased expression of RPE65 (2.22, 2.61, 2.97 folds respectively), CRALBP (1.78, 1.45,1.87 folds) and complement associated gene especially CD46 (2.93, 2.95, 3.41 folds) in comparison to the untreated control ($P < 0.05$). Two hours incubation of fRPE with ATRA in concentrations of 10^{-6} M and 10^{-7} M did not increase gene expression levels of bestrophin (0.78, 0.92 folds), while ATRA in lower concentration (10^{-8} M) could increase bestrophin expression (1.40 folds) ($P < 0.05$) in 2 hours. In contrast, after incubating fRPE with ATRA for 24 hours, the expression levels of RPE65 (0.24, 0.29, 0.93 folds), bestrophin (0.33, 0.39, 0.55 folds) and CRALBP (0.56, 0.45, 0.77 folds) were decreased. The upregulated effects of RPE related marks with 2-hour RA incubation was also observed in the hESC-RPE. Treating hESC-RPE with RA in all tested concentrations for 24 hours, the expression levels of RPE65 decreased,while, the expression levels of BEST (1.89, 1.59, 1.70 folds) and CRALBP (2.38, 2.57, 3.21 folds) were still upregulated ($P < 0.05$) (Fig. 5A-C). Interestingly, treating hiPSC-RPE cells with 10^{-7} M RA for either 2 hours or 24 hours, the expression levels of RPE65, BEST and CRALBP genes were all upregulated.

We detected the changes of complement negative regulatory proteins (CRPs) including complement factor H (CFH), CD46, CD55 and CD59 as well. Incubating with ATRA at different concentrations for 2 hours or 24 hours, the expression levels of CRPs in all three RPE cell types were enhanced mostly, except that the expression levels of CD46, CD55 and CD56 in hiPSC-RPE showed different trends after being incubated with ATRA at concentration of 10^{-8} for 24 hours (Fig. 5D-F).

According to the results of RT-PCR, we chose 10^{-7}M RA as the concentration of treatment in the following immunocytochemistry and western blot test. As shown here, after incubating with 10^{-7} M RA for 2 hours, the expression of RPE markers and CRPs in three types of RPE cells increased in various degree (Fig. 6A, Fig. 7). fRPE cultured for longer duration (3 months) had higher CRALBP expression levels compared with the cells cultured for 2 months. However, the expression level of bestrophin did not increase with longer culturing duration. ATRA incubation also did not improve the expression level of bestrophin in fRPE cells, but could improve the expression level of CRALBP (Fig. 6B)

Effect of ATRA on TER in fRPE, hESC-RPE and iPSC-RPE

TER was measured in P3 fRPE, hESC-RPE and hiPSC-RPE which had been cultured for more than one month and sequentially incubated with RPE medium containing 10^{-7} M of ATRA for two more weeks. The average TER of P3 fRPE cultured for 6 weeks without ATRA was 1559.92 ± 237.77 Ωcm^2, much higher than those of P3 hESC-RPE (243.83 ± 32.16 Ωcm^2) and P3 hiPSC-RPE (336.58 ± 29.09 Ωcm^2). Incubation with 10^{-7} M of ATRA for two weeks could increase TERs significantly among fRPE (1849.17 ± 137.03 Ωcm^2), hESC-RPE (282.33 ± 12.44 Ωcm^2) and hiPSC-RPE cells (379.83 ± 37.37 Ωcm^2) (Fig. 8). Results showed that TERs of stem cell-derived RPE were significantly lower than those of the fRPE with or without RA treatment ($P < 0.0001$), while there were no significant differences in TERs between hESC-RPE and hiPSC-RPE (control: $P = 0.1764$, ATRA treated cells: $P = 0.1428$).

Discussion

Over the past decade, RPE cell transplantation has been explored as a useful treatment to replace the damaged cells and improve visual function in degenerated retinal diseases. Scientists investigated methods to culture and expand fRPE for cell-based transplantation in human eyes with AMD [28, 29]. However, fetal RPE cell lines are difficult to obtain. Subsequently, RPE cells derived from ESCs and iPSCs, which have tremendous potential to expand *in vitro*, have been proposed as new sources for RPE transplantation [27, 29–33]. Dr. Schwartz *et al* [7, 34] successfully transplanted hESC-RPE cell suspension into subretinal space of patients with AMD or Stargardt. More than half of the treated patients were reported to have sustained improvements in visual acuity, although the absolute level of visual acuity was quite low. In 2014, the world's first autologous iPSC-derived RPE transplant was carried out by the Riken Center for Developmental Biology in Japan, and no initial safety concerns were reported so far by now [35].

One prerequisite for the RPE subretinal transplantation is that the donor RPE cells from different sources should exhibit similar characteristics of the RPE in *vivo*, to ensure that the transplanted cells can play normal functions in subretinal space. Zhang Q at al demonstrated that highly differentiated human fetal RPE cultures had more resistance to the accumulation and toxicity of lipofuscin-like material [36]. Ever since Gouras and Hu DN established the primary cultured RPE cell line in the early 1980s [37, 38], methods for culturing RPE have been modified and improved over 40 years. However, there are still unsolved problems in maintaining the long-term characters and function of cultured RPE effectively. The tendency of RPE cells undergoing a lasting switch to a mesenchymal state may compromise the outcome of cell transplantation [39, 40], and may cause unexpectable complications such as proliferative vitreoretinopathy (PVR). Our results suggested that RPE cells plated at higher densities could maintain polygonal, cobblestone-like RPE morphology, while cells seeded at lower densities could trigger EMT changes. In addition, RPE cells with higher passage number or handled with inappropriate digesting methods underwent EMT changes and lost RPE morphology and pigmentation. The mesenchymal fRPE and stem cell-derived RPE expressed less epithelial differentiation markers including E-cadherin, ZO-1 and RPE65, gained the mesenchymal markers including α-SMA, N-cadherin and FN at both gene and protein levels. Singh R *et al* tested the effects of serial expansion on the cellular, molecular, and functional properties of hiPSC-derived RPE cultures [20]. They found that expansion of hiPSC-RPE monolayers over the first three passages resulted in decreased expression of pluripotency and neuroretinal markers, and maintained characteristic morphological features and gene and protein expression profiles. In contrast, P4 hiPSC-RPE cells failed to form monolayers and possessed altered morphological and functional characteristics and gene expression levels. However, our study proved that P4 RPE of all three types seeded at a density of 6×10^5 and 9×10^5 cells/mL in basal medium maintained typical RPE morphology and gene expression profiles. The discrepancy may be explained by the lower plating density used in Singh's study. They passaged hiPSC-RPE onto inserts at a density of 20,000 cells per 6.5-mm Tran swell, which his much lower than the standard density of 6×10^5 cells/mL we proved to have the ability to maintain RPE features over serial passaging. We also found that the dissociating method was also very important to maintain passaged RPE cells with high quality. These findings highlight the importance to develop standard methods of cultivating, passaging and manipulating fRPE, hESC-derived RPE and hiPSC-derived RPE cells in vitro for future cell-based transplantation.

Liao JL et al demonstrated that functional hESC-derived RPE cells can exhibit cobblestone-like morphology, pigment synthesis and vitamin A phagocytic function similar to fRPE cells [41]. In our study, hESC line was successfully differentiated into RPE-like cells. However, we found that hESC-RPE cells in vitro also underwent EMT with low plating density, repeat passaging and inappropriate digesting methods. Gene and protein expression changes in mesenchymal stem cells-derived RPE matched with those of fRPE cells. Interestingly, we found there were some differences between stem cell-derived RPE and fRPE when cells underwent EMT. The expression of E-cadherin increased after EMT changes in stem cells derived RPE, which was downregulated in mesenchymal fRPE. Liao JL et al [41] found that there are 87 genes expressed in fRPE and only about 2/3 were expressed in hESC-RPE, 21 genes that were specific for fRPE had no expression in hESC-RPE by global gene expression analysis. The cause of E-cadherin

expression upregulated in hESC-RPE cells undergoing EMT in this study also implied that although stem cell-derived RPE cells are morphologically similar to fRPE cells, there are differences in gene expressions and functionalities among different RPE cell types.

Morphological changes and pigmentation do not represent all RPE functionalities. RPE plays complex roles, especially a major role in controlling the ocular immune response through expression of various CRPs during the pathological process of AMD and Stargardts disease. Photoreceptors are critically dependent on a healthy RPE for continued viability [42]. CRPs such as CD46, CD55, and CD59, protect host cells from complement attack. CRPs in RPE cell are upregulated by inflammatory cytokines and repetitive nonlethal oxidant exposure in a species-specific manner. Increased CRPs expression may help to protect RPE cells from complement- and oxidant-mediated injury in AMD [43]. Our results showed that stem cell-derived RPE cells have compromised CRPs expression compared with fRPE cells. It may be as important as to obtain well differentiated stem cells derived RPE cells with comparable CRPs expression as RPE markers for cell-based therapy.

Retinoic acid (RA) derivatives from vitamin A are involved in a number of biological processes, e.g. vision, embryogenesis, cell differentiation of blood cells, as well as of skin and tumor cells [44, 45]. RA signaling promotes normal development of the ventral retina and optic nerve through its activities in the neural crest cell-derived periocular mesenchyme [21]. Studies showed that ATRA administration could upregulate ciliary neurotrophic factor (CNTF, a trophic factor that promotes rod and cone photoreceptor survival and cone outer segment regeneration in the degenerating retina) expression in RPE cells [46]. ATRA could inhibit proliferation of RPE from the Proliferative Vitreoretinopathy (PVR) membrane [47], increase melanin synthesis in a time-dependent manner in vitro [48], inhibit RPE cell-mediated collagen gel contraction [49], promote the epithelial barrier function in vitro, which is accompanied by altering expression of tight junctions (TJ)-associated proteins [50]. In this study, after treating fRPE with RA at all three selected concentrations for 2 h, the expression levels of RPE65, BEST and CRALBP increased significantly, and decreased slightly after incubation of RA extended to 24 hours. However, the overall expression levels of RPE65, BEST and CRALBP were still much higher than those of hESC-RPE and iPSC-RPE cells (data not shown here). ATRA promoted the expression of RPE-specific genes at all tested concentrations after 2-hour incubation in hESC-RPE cells and enhanced CRPs expression after 24 hours incubation. ATRA greatly enhanced CRPs expression iPSC-RPE at all concentrations after incubating for 2 hours and promoted RPE-specific genes expression at a concentration of 10^{-7}M. ATRA promoted the expression of CRPs genes in three kinds of RPE cells at all concentrations tested in this study, indicating that ATRA may be used as an adjuvant drug for RPE cell transplantation to enhance its complement function.

Our study also proved that incubating P4 fRPE, hESC-RPE and hiPSC-RPE with ATRA could enhance transepithelial resistance. TERs of stem cell-derived RPE were significantly lower than those of the fRPE with or without RA treatment, while there were no significant difference in TERs between hESC-RPE and hiPSC-RPE. However, in Singh R's study, TERs in fRPE were lower than the hiPSC-derived RPE [20]. The mean TER values of hiPSC-derived RPE in our study were 379.83 ± 37.37 Ωcm^2, which was very close to

the TER values in Singh's study (P1:355.9 ± 48.9 Ωcm^2, P2: 451.7 ± 16.0 Ωcm^2, P3: 394.6 ± 16.0 Ωcm^2) and the values in other studies, while, the mean TER values of fRPE in our study (1559.92 ± 237.77 Ωcm^2) were much higher than those of fRPE in Singh's study (359.5 ± 15.0 Ωcm^2), but similar to the results of Liu Z's study (1,247 ± 107.7 $\Omega \cdot cm^2$) [51]. These discrepancies, again, highlight that the methods of generating and cultivating fRPE and stem cells derived RPE have great impacts on the cell quality and the performance of those cells.

In summary, our study demonstrates that stem cells derived RPE cells also have the tendency to undergo EMT changes during the culturing and passaging process in *vitro*. Moreover, ATRA can increase RPE markers expression in fRPE cells and stem cells derived RPE cells, as well as to increase the expression levels of CRPs and transepithelial resistance. However, this study has limitations. We did not observe long term effects of ATRA on fRPE cells and stem cells derived RPE cells, and we did not compare the performance of the three types of RPE cells in *vivo*. Therefore, further experiments seem warranted to extend the effective lifespan of RPE and explore better strategy to differentiate stem cells into mature RPE cells with proper functionalities. Gold standards of maturation features of donor stem cells derived RPE cells should be set up to ensure optimal outcome of cell transplantation.

Conclusion

In summary, our work demonstrated that RPE cells from different sources may undergo mesenchymal changes during the process of culturing and serial expanding in *vitro.* Moreover, ATRA may be used as an adjuvant treatment to induce differentiation and maturation of fRPE and stem cell-derived RPE cells for successful cell-based therapy.

Abbreviations

fRPE: fetal retinal pigment epithelium; hESC: human embryonic stem cell; hiPSC: human induced pluripotent stem cell; ATRA: all-trans retinoic acid; RA: retinoic acid; CRP: complement regulatory proteins; CFH: complement factor H; TER: transepithelial resistance; EMT: epithelial-to-mesenchymal transition; AMD: age-related macular degeneration; VEGF: vascular endothelial growth factor; P: passage; HPV: human papilloma virus; MEF: mouse embryonic fibroblast; FBS: fatal bovine serum; NEAA: Non-essential amino acids; bFGF: basic fibroblast growth factor; PBS: phosphate-buffered saline; RT-PCR: real time PCR; AP: alkaline phosphatase; BEST: bestrophin; PVR: proliferative vitreoretinopathy.

Declarations

Acknowledgements

We wish to thank Dr. Neil Bressler from John Hopkins University for reviewing the manuscript. We thank Prof. Tao Meng from the First Affiliated Hospital of China Medical university for helping the tissue donation and Prof. Weidong Li from Shanghai Jiaotong University for providing cells.

Consent for publication

Not applicable

Funding

This work was supported by Liaoning Guangfu Hereditary Eye Disease Philanthropic Foundation (No. #2900020001).

Authors' contributions:

TY and NY carried out the collection and/or assembly of data, manuscript writing, data analysis and interpretation. WH participated in the collection and/or assembly of data, data analysis and interpretation. XZ participated the data analysis and interpretation. XL carried out the provision of study material or patients. YW participated in the data analysis and interpretation. JK carried out the conception and design, financial support and final approval of manuscript. All authors read and approved the final manuscript. (TY-Y and N-Y contributed equally.)

Availability of data and materials

The datasets used in this study are available from the corresponding author on reasonable request, and all generated data are included in the article and its additional files.

Ethics approval and consent to participate

All procedures performed in studies were in accordance with the ethical standards of the Affiliated Hospital of China Medical University and with the 1964 Helsinki Declaration. Written informed consent for the use of the tissue was obtained.

Competing interests

The authors declare that they have no competing interests.

References

1. Zhou, M., Duan, P., Liang, J., Zhang, X. & Pan, C. Geographic distributions of age-related macular degeneration incidence: a systematic review and meta-analysis. *The British journal of ophthalmology* (2020).

2. Mitchell, P., Liew, G., Gopinath, B. & Wong, T. Age-related macular degeneration. *Lancet (London, England)* **392**, 1147-1159 (2018).
3. Jager, R., Mieler, W. & Miller, J. Age-related macular degeneration. *The New England journal of medicine* **358**, 2606-2617 (2008).
4. Lynch, A. et al. Systemic activation of the complement system in patients with advanced age-related macular degeneration. *European journal of ophthalmology* **30**, 1061-1068 (2020).
5. Genead, M., Fishman, G., Stone, E. & Allikmets, R. The natural history of stargardt disease with specific sequence mutation in the ABCA4 gene. *Investigative ophthalmology & visual science* **50**, 5867-5871 (2009).
6. Sears, A. et al. Towards Treatment of Stargardt Disease: Workshop Organized and Sponsored by the Foundation Fighting Blindness. *Translational vision science & technology* **6**, 6 (2017).
7. Schwartz, S. et al. Human embryonic stem cell-derived retinal pigment epithelium in patients with age-related macular degeneration and Stargardt's macular dystrophy: follow-up of two open-label phase 1/2 studies. *Lancet (London, England)* **385**, 509-516 (2015).
8. Song, W. et al. Treatment of macular degeneration using embryonic stem cell-derived retinal pigment epithelium: preliminary results in Asian patients. *Stem cell reports* **4**, 860-872 (2015).
9. Zhong, X. et al. Generation of three-dimensional retinal tissue with functional photoreceptors from human iPSCs. *Nature communications* **5**, 4047 (2014).
10. Phillips, M. et al. Blood-derived human iPS cells generate optic vesicle-like structures with the capacity to form retinal laminae and develop synapses. *Investigative ophthalmology & visual science* **53**, 2007-2019 (2012).
11. Garber, K. RIKEN suspends first clinical trial involving induced pluripotent stem cells. *Nature biotechnology* **33**, 890-891 (2015).
12. Sugino, I. et al. Comparison of FRPE and human embryonic stem cell-derived RPE behavior on aged human Bruch's membrane. *Investigative ophthalmology & visual science* **52**, 4979-4997 (2011).
13. Chichagova, V. et al. Cellular regeneration strategies for macular degeneration: past, present and future. *Eye (London, England)* **32**, 946-971 (2018).
14. Lu, Y. et al. A comparison of autologous transplantation of retinal pigment epithelium (RPE) monolayer sheet graft with RPE-Bruch's membrane complex graft in neovascular age-related macular degeneration. *Acta ophthalmologica* **95**, e443-e452 (2017).
15. Mandai, M. et al. Autologous Induced Stem-Cell-Derived Retinal Cells for Macular Degeneration. *The New England journal of medicine* **376**, 1038-1046 (2017).
16. Reichman, S. et al. Generation of Storable Retinal Organoids and Retinal Pigmented Epithelium from Adherent Human iPS Cells in Xeno-Free and Feeder-Free Conditions. *Stem cells (Dayton, Ohio)* **35**, 1176-1188 (2017).
17. Hjelmeland, L., Fujikawa, A., Oltjen, S., Smit-McBride, Z. & Braunschweig, D. Quantification of retinal pigment epithelial phenotypic variation using laser scanning cytometry. *Molecular vision* **16**, 1108-

1121 (2010).

18. Cao, S., Walker, G., Wang, X., Cui, J. & Matsubara, J. Altered cytokine profiles of human retinal pigment epithelium: oxidant injury and replicative senescence. *Molecular vision* **19**, 718-728 (2013).
19. Hu, J. & Bok, D. The use of cultured human fetal retinal pigment epithelium in studies of the classical retinoid visual cycle and retinoid-based disease processes. *Experimental eye research* **126**, 46-50 (2014).
20. Singh, R. et al. Functional analysis of serially expanded human iPS cell-derived RPE cultures. *Investigative ophthalmology & visual science* **54**, 6767-6778 (2013).
21. Cvekl, A. & Wang, W. Retinoic acid signaling in mammalian eye development. *Experimental eye research* **89**, 280-291 (2009).
22. Zhang, D. et al. All-trans retinoic acid stimulates the secretion of TGF-β2 via the phospholipase C but not the adenylyl cyclase signaling pathway in retinal pigment epithelium cells. *BMC ophthalmology* **19**, 23 (2019).
23. Wang, S., Liu, S., Mao, J. & Wen, D. Effect of retinoic acid on the tight junctions of the retinal pigment epithelium-choroid complex of guinea pigs with lens-induced myopia in vivo. *International journal of molecular medicine* **33**, 825-832 (2014).
24. Mao, J. & Liu, S. Regulation of RPE barrier function by all-trans retinoic acid in myopia. *Neuroscience letters* **568**, 17-22 (2014).
25. Creek, K. et al. Retinoic acid suppresses human papillomavirus type 16 (HPV16)-mediated transformation of human keratinocytes and inhibits the expression of the HPV16 oncogenes. *Advances in experimental medicine and biology* **354**, 19-35 (1994).
26. Maminishkis, A. et al. Confluent monolayers of cultured human fetal retinal pigment epithelium exhibit morphology and physiology of native tissue. *Investigative ophthalmology & visual science* **47**, 3612-3624 (2006).
27. Buchholz, D. et al. Derivation of functional retinal pigmented epithelium from induced pluripotent stem cells. *Stem cells (Dayton, Ohio)* **27**, 2427-2434 (2009).
28. Algvere, P., Berglin, L., Gouras, P., Sheng, Y. & Kopp, E. Transplantation of RPE in age-related macular degeneration: observations in disciform lesions and dry RPE atrophy. *Graefe's archive for clinical and experimental ophthalmology = Albrecht von Graefes Archiv fur klinische und experimentelle Ophthalmologie* **235**, 149-158 (1997).
29. Hirano, M. et al. Generation of structures formed by lens and retinal cells differentiating from embryonic stem cells. *Developmental dynamics : an official publication of the American Association of Anatomists* **228**, 664-671 (2003).
30. Kawasaki, H. et al. Generation of dopaminergic neurons and pigmented epithelia from primate ES cells by stromal cell-derived inducing activity. *Proceedings of the National Academy of Sciences of the United States of America* **99**, 1580-1585 (2002).
31. Klimanskaya, I. et al. Derivation and comparative assessment of retinal pigment epithelium from human embryonic stem cells using transcriptomics. *Cloning and stem cells* **6**, 217-245 (2004).

32. Meyer, J. et al. Modeling early retinal development with human embryonic and induced pluripotent stem cells. *Proceedings of the National Academy of Sciences of the United States of America* **106**, 16698-16703 (2009).
33. Carr, A. et al. Protective effects of human iPS-derived retinal pigment epithelium cell transplantation in the retinal dystrophic rat. *PloS one* **4**, e8152 (2009).
34. Schwartz, S. et al. Embryonic stem cell trials for macular degeneration: a preliminary report. *Lancet (London, England)* **379**, 713-720 (2012).
35. Kamao, H. et al. Characterization of human induced pluripotent stem cell-derived retinal pigment epithelium cell sheets aiming for clinical application. *Stem cell reports* **2**, 205-218 (2014).
36. Zhang, Q. et al. Highly Differentiated Human Fetal RPE Cultures Are Resistant to the Accumulation and Toxicity of Lipofuscin-Like Material. *Investigative ophthalmology & visual science* **60**, 3468-3479 (2019).
37. Flood, M., Gouras, P. & Kjeldbye, H. Growth characteristics and ultrastructure of human retinal pigment epithelium in vitro. *Investigative ophthalmology & visual science* **19**, 1309-1320 (1980).
38. Hu, D., Del Monte, M., Liu, S. & Maumenee, I. Morphology, phagocytosis, and vitamin A metabolism of cultured human retinal pigment epithelium. *Birth defects original article series* **18**, 67-79 (1982).
39. Lee, S. et al. Epitheliomesenchymal transdifferentiation of cultured RPE cells. *Ophthalmic research* **33**, 80-86 (2001).
40. Tamiya, S. & Kaplan, H. Role of epithelial-mesenchymal transition in proliferative vitreoretinopathy. *Experimental eye research* **142**, 26-31 (2016).
41. Liao, J. et al. Molecular signature of primary retinal pigment epithelium and stem-cell-derived RPE cells. *Human molecular genetics* **19**, 4229-4238 (2010).
42. Lenis, T. et al. Complement modulation in the retinal pigment epithelium rescues photoreceptor degeneration in a mouse model of Stargardt disease. *Proceedings of the National Academy of Sciences of the United States of America* **114**, 3987-3992 (2017).
43. Yang, P., Tyrrell, J., Han, I. & Jaffe, G. Expression and modulation of RPE cell membrane complement regulatory proteins. *Investigative ophthalmology & visual science* **50**, 3473-3481 (2009).
44. Evans, T. & Kaye, S. Retinoids: present role and future potential. *British journal of cancer* **80**, 1-8 (1999).
45. Axel, D. et al. All-trans retinoic acid regulates proliferation, migration, differentiation, and extracellular matrix turnover of human arterial smooth muscle cells. *Cardiovascular research* **49**, 851-862 (2001).
46. Zhou, W. et al. All-trans retinoic acid upregulates the expression of ciliary neurotrophic factor in retinal pigment epithelial cells. *Cell biochemistry and function* **35**, 202-208 (2017).
47. Wu, W., Hu, D., Mehta, S. & Chang, Y. Effects of retinoic acid on retinal pigment epithelium from excised membranes from proliferative vitreoretinopathy. *Journal of ocular pharmacology and therapeutics : the official journal of the Association for Ocular Pharmacology and Therapeutics* **21**, 44-54 (2005).

48. Kishi, H., Mishima, H. & Yamashita, U. Effects of retinoic acid and TGF-beta 1 on the proliferation and melanin synthesis in chick retinal pigment epithelial cells in vitro. *Current eye research* **17**, 483-486 (1998).
49. Chang, Y., Kao, Y., Hu, D., Tsai, L. & Wu, W. All-trans retinoic acid remodels extracellular matrix and suppresses laminin-enhanced contractility of cultured human retinal pigment epithelial cells. *Experimental eye research* **88**, 900-909 (2009).
50. Rong, J. & Liu, S. Effect of all-trans retinoic acid on the barrier function in human retinal pigment epithelial cells. *Biochemical and biophysical research communications* **407**, 605-609 (2011).
51. Liu, Z., Meyer, C. & Stanzel, B. Effect of novel vital dyes on outer blood-retina barrier function in cultured human retinal pigment epithelium. *Ophthalmologica. Journal international d'ophtalmologie. International journal of ophthalmology. Zeitschrift fur Augenheilkunde*, 33-40 (2013).

Figures

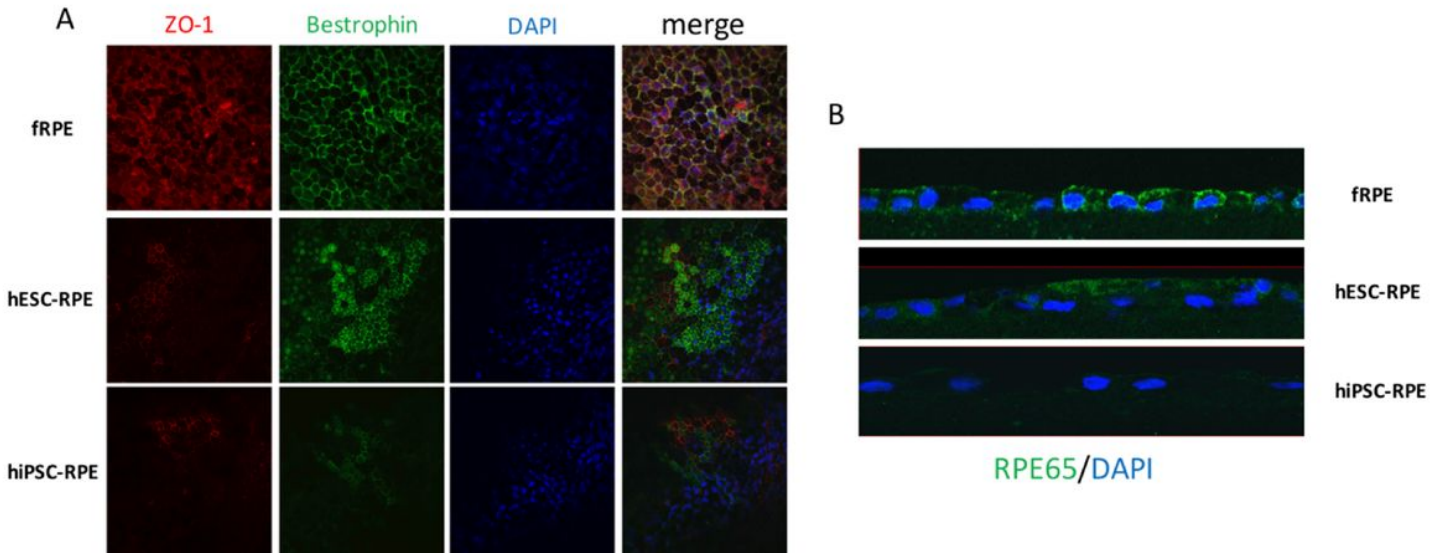

Figure 1

Immunofluorescent labeling of RPE-signature proteins expression in fRPE, hESC-RPE and hiPSC-RPE. After being cultured for 2 months, RPE cells from different sources showed robust expression of RPE signature proteins, including RPE65 (B), Bestrophin and ZO-1 (A). The expressions of RPE related markers were more robust in fRPE cells than those of stem cells derived RPE cells. hiPSC-RPE cells showed weakest expression of RPE markers among the three types of RPE cells.

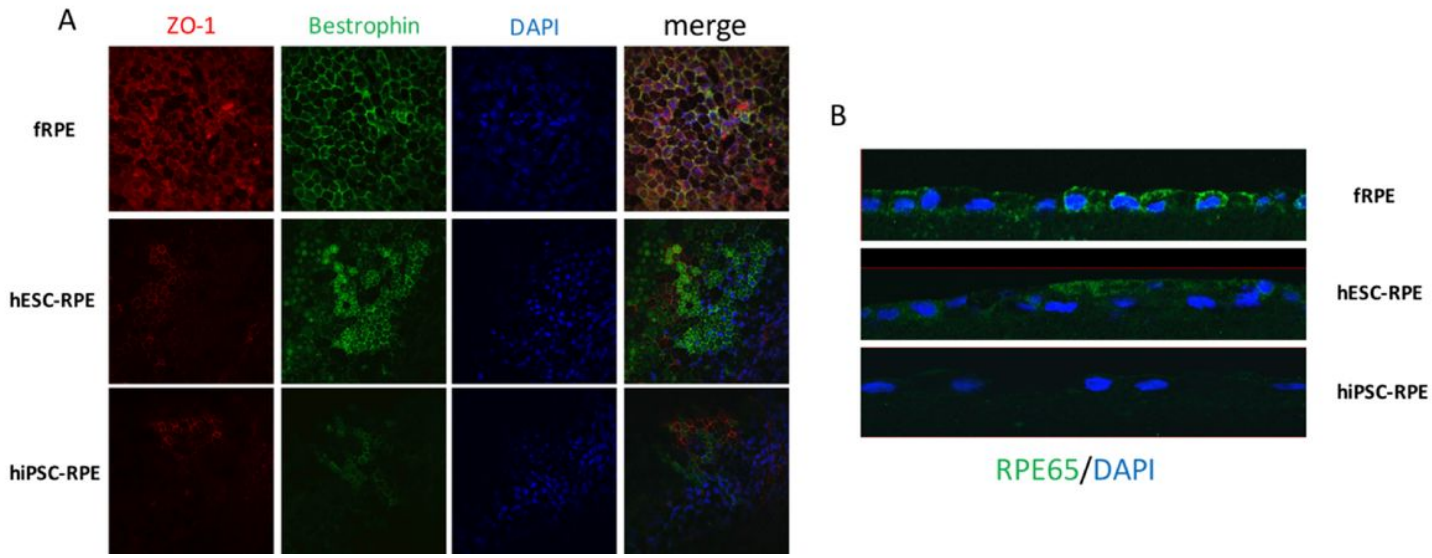

Figure 1

Immunofluorescent labeling of RPE-signature proteins expression in fRPE, hESC-RPE and hiPSC-RPE. After being cultured for 2 months, RPE cells from different sources showed robust expression of RPE signature proteins, including RPE65 (B), Bestrophin and ZO-1 (A). The expressions of RPE related markers were more robust in fRPE cells than those of stem cells derived RPE cells. hiPSC-RPE cells showed weakest expression of RPE markers among the three types of RPE cells.

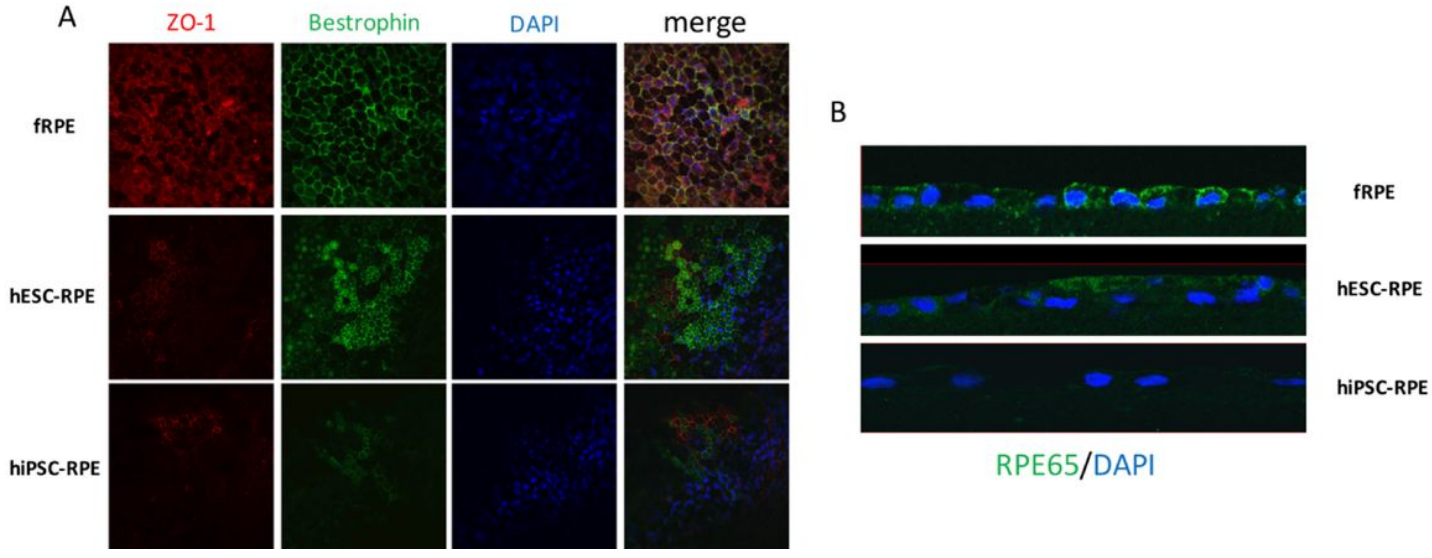

Figure 1

Immunofluorescent labeling of RPE-signature proteins expression in fRPE, hESC-RPE and hiPSC-RPE. After being cultured for 2 months, RPE cells from different sources showed robust expression of RPE signature proteins, including RPE65 (B), Bestrophin and ZO-1 (A). The expressions of RPE related markers were more robust in fRPE cells than those of stem cells derived RPE cells. hiPSC-RPE cells showed weakest expression of RPE markers among the three types of RPE cells.

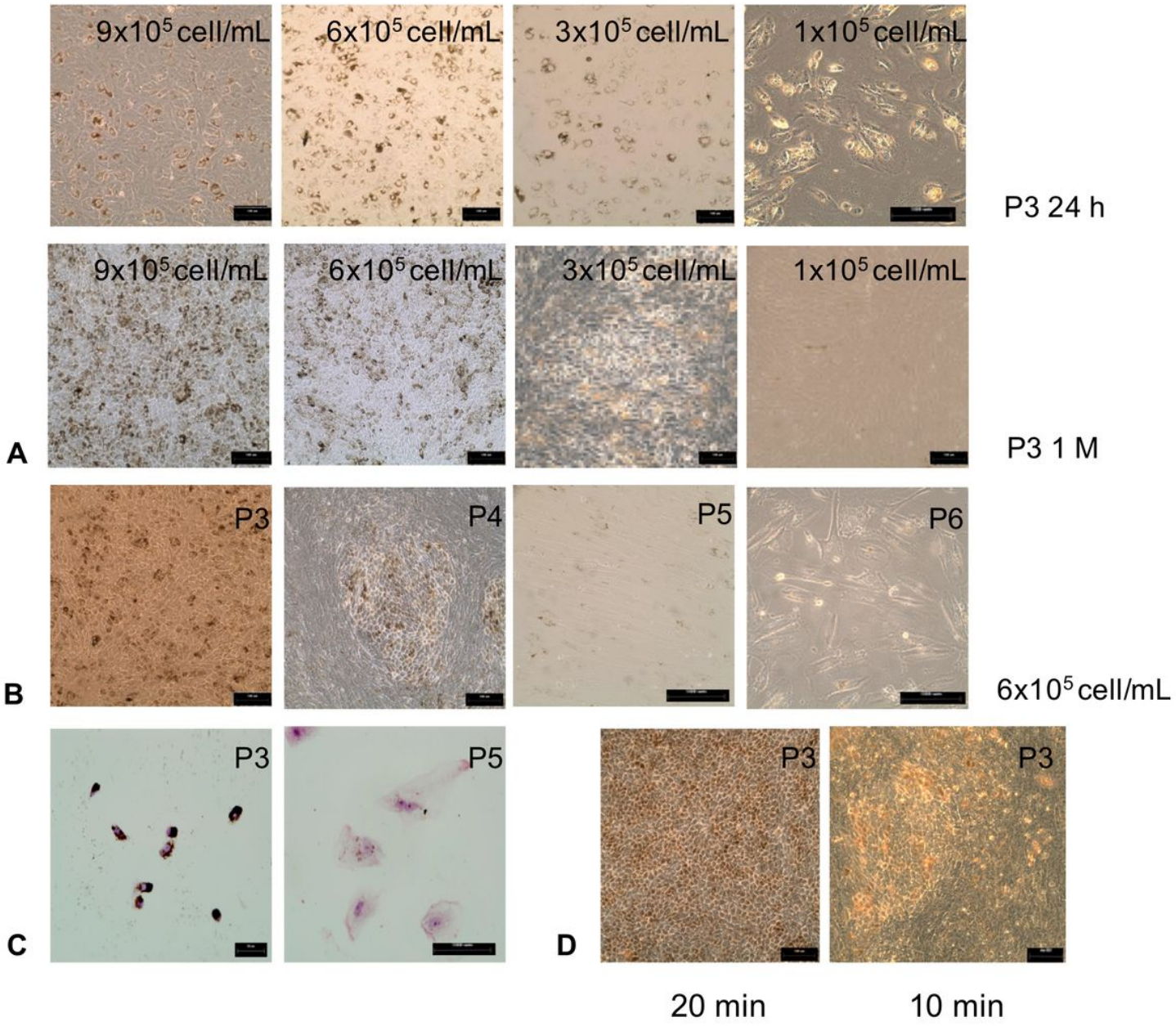

Figure 2

Effects of cultural conditions on cell morphology of fRPE. (A): Effects of different passaging densities on RPE morphology. (A1-2) Results revealed P3 fRPE cells passaged at density of 9x105 cells/mL and 6x105 cells/mL expanded to form confluent sheets and exhibited polygonal, cobblestone-like morphology after being plated for 24 hours; (A3-4) P3 fRPE passaged at lower densities of 1x105 cells/mL and 3x105 cells/mL exhibited fibroblast-like morphology with increased size; (A5-6) After being cultured for 1 month, P3 fRPE cells plated at higher density showed heavy pigmentation; (A7) P3 fRPE cells plated at a density of 3×105 cells/mL exhibited fusiform and disorganized shapes; (A8) P3 fRPE cells plated at a density of 1x105 cells/mL showed characteristics of mesenchymal cells without pigmentation; (B): Effects of different passage number on RPE morphology. (B1) fRPE could maintain typical RPE morphology and heavy pigmentation till P3; (B2) P4 fRPE showed less pigmentation; (B3) P5 fRPE still behaved cellular fusion with little pigmentation; (B4) P6 fRPE had abundant characteristics of mesenchymal cells without

pigmentation and cellular fusion; (C): Hematoxylin-Eosin (HE) Staining of P3 and P5 fRPE after being plated for 24 hours. (C1) P3 fRPE exhibited polygonal, cobblestone-like morphology with melanosome granules; (C2) P5 fRPE showed spindle shape with less pigmentation; (D): Effects of dissociating time on RPE morphology. P3 fRPE cells plated at 6x105cells/mL were cultured for 1 month. (D1) P3 fRPE dissociated by 0.25% trypsin for 30-40 minutes maintained polygonal, cobblestone-like morphology and heavy pigmentation; (D2) P3 fRPE dissociated for 10-20 minutes started to exhibit fibroblast-like morphology indicating that inappropriate passaging methods led to mesenchymal changes.

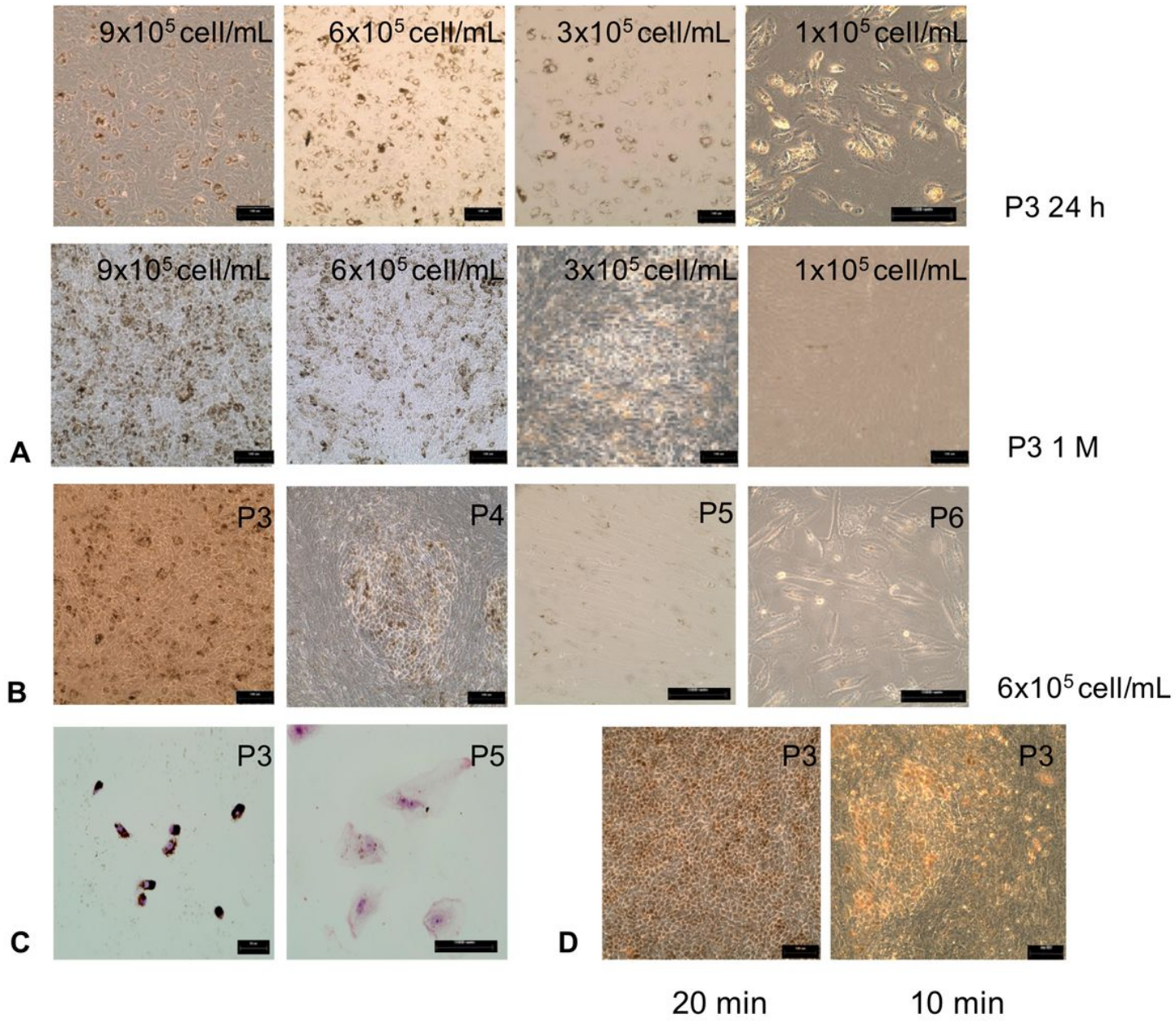

Figure 2

Effects of cultural conditions on cell morphology of fRPE. (A): Effects of different passaging densities on RPE morphology. (A1-2) Results revealed P3 fRPE cells passaged at density of 9x105 cells/mL and 6x105 cells/mL expanded to form confluent sheets and exhibited polygonal, cobblestone-like morphology after being plated for 24 hours; (A3-4) P3 fRPE passaged at lower densities of 1x105 cells/mL and 3x105

cells/mL exhibited fibroblast-like morphology with increased size; (A5-6) After being cultured for 1 month, P3 fRPE cells plated at higher density showed heavy pigmentation; (A7) P3 fRPE cells plated at a density of 3×105 cells/mL exhibited fusiform and disorganized shapes; (A8) P3 fRPE cells plated at a density of 1x105 cells/mL showed characteristics of mesenchymal cells without pigmentation; (B): Effects of different passage number on RPE morphology. (B1) fRPE could maintain typical RPE morphology and heavy pigmentation till P3; (B2) P4 fRPE showed less pigmentation; (B3) P5 fRPE still behaved cellular fusion with little pigmentation; (B4) P6 fRPE had abundant characteristics of mesenchymal cells without pigmentation and cellular fusion; (C): Hematoxylin-Eosin (HE) Staining of P3 and P5 fRPE after being plated for 24 hours. (C1) P3 fRPE exhibited polygonal, cobblestone-like morphology with melanosome granules; (C2) P5 fRPE showed spindle shape with less pigmentation; (D): Effects of dissociating time on RPE morphology. P3 fRPE cells plated at 6x105cells/mL were cultured for 1 month. (D1) P3 fRPE dissociated by 0.25% trypsin for 30-40 minutes maintained polygonal, cobblestone-like morphology and heavy pigmentation; (D2) P3 fRPE dissociated for 10-20 minutes started to exhibit fibroblast-like morphology indicating that inappropriate passaging methods led to mesenchymal changes.

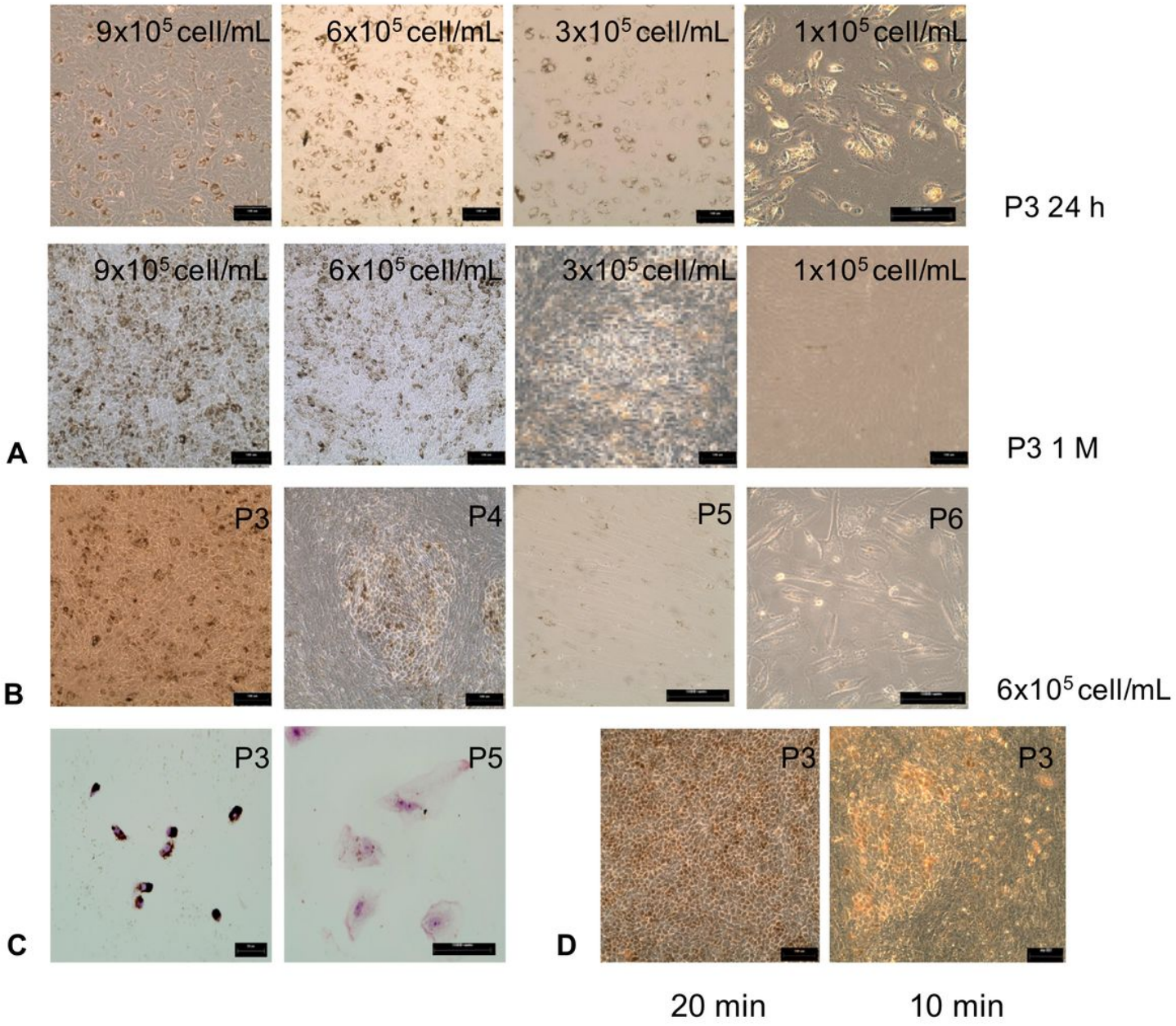

Figure 3

Effects of cultural conditions on cell morphology of fRPE. (A): Effects of different passaging densities on RPE morphology. (A1-2) Results revealed P3 fRPE cells passaged at density of 9x105 cells/mL and 6x105 cells/mL expanded to form confluent sheets and exhibited polygonal, cobblestone-like morphology after being plated for 24 hours; (A3-4) P3 fRPE passaged at lower densities of 1x105 cells/mL and 3x105 cells/mL exhibited fibroblast-like morphology with increased size; (A5-6) After being cultured for 1 month, P3 fRPE cells plated at higher density showed heavy pigmentation; (A7) P3 fRPE cells plated at a density of 3×105 cells/mL exhibited fusiform and disorganized shapes; (A8) P3 fRPE cells plated at a density of 1x105 cells/mL showed characteristics of mesenchymal cells without pigmentation; (B): Effects of different passage number on RPE morphology. (B1) fRPE could maintain typical RPE morphology and heavy pigmentation till P3; (B2) P4 fRPE showed less pigmentation; (B3) P5 fRPE still behaved cellular fusion with little pigmentation; (B4) P6 fRPE had abundant characteristics of mesenchymal cells without

pigmentation and cellular fusion; (C): Hematoxylin-Eosin (HE) Staining of P3 and P5 fRPE after being plated for 24 hours. (C1) P3 fRPE exhibited polygonal, cobblestone-like morphology with melanosome granules; (C2) P5 fRPE showed spindle shape with less pigmentation; (D): Effects of dissociating time on RPE morphology. P3 fRPE cells plated at 6x105cells/mL were cultured for 1 month. (D1) P3 fRPE dissociated by 0.25% trypsin for 30-40 minutes maintained polygonal, cobblestone-like morphology and heavy pigmentation; (D2) P3 fRPE dissociated for 10-20 minutes started to exhibit fibroblast-like morphology indicating that inappropriate passaging methods led to mesenchymal changes.

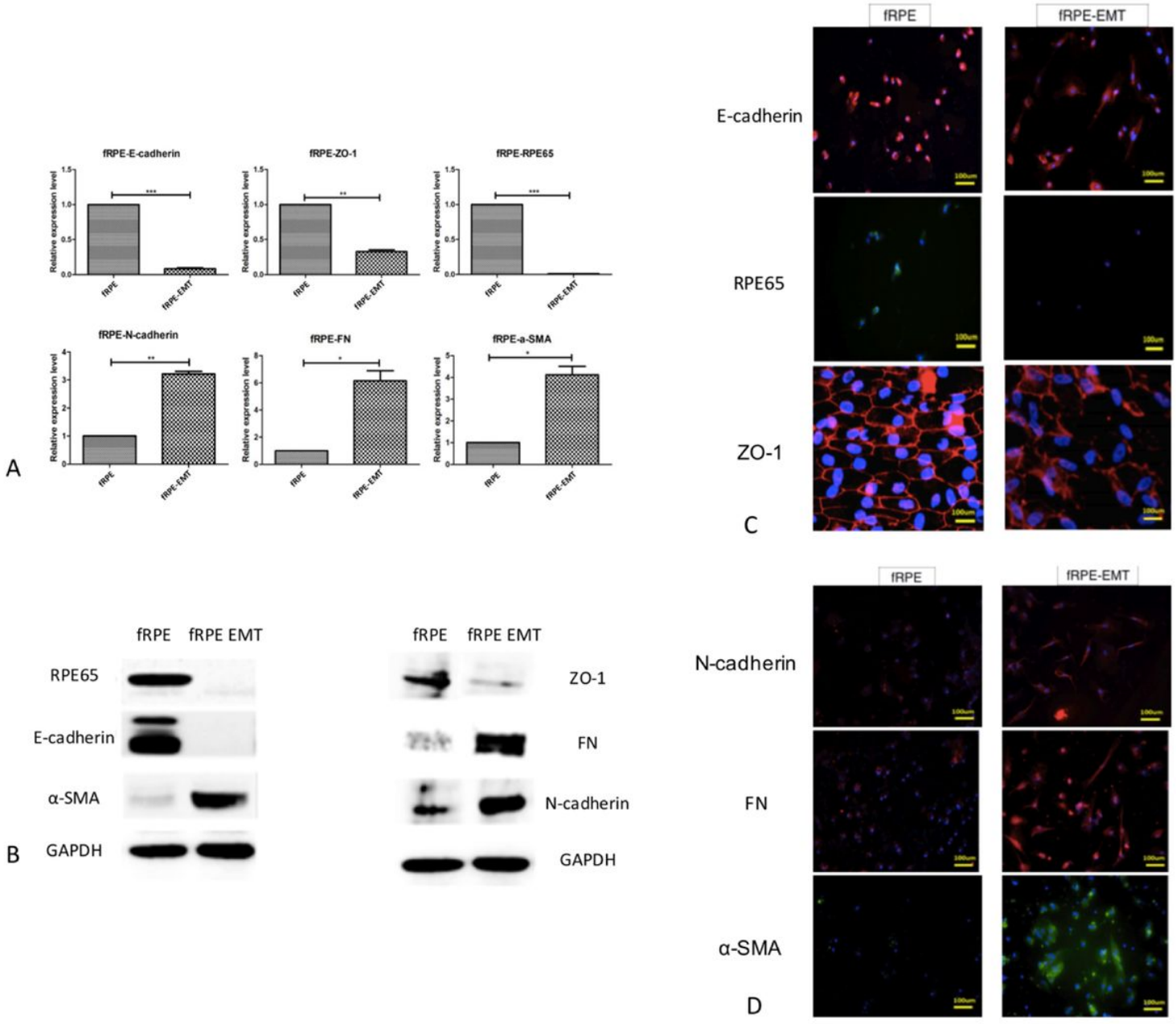

Figure 3

Expression of RPE-specific markers and mesenchymal markers EMT in fRPE.(A) RT–qPCR analysis of RPE-specific markers and mesenchymal markers in fRPE with or without EMT changes: It showed that RPE65, E-cadherin and ZO-1 expression in fRPE cells undergone EMT changes were significantly

decreased and a-SMA, N-cadherin and FN were significantly increased by 4.12 folds, 3.21 folds and 10.26 folds respectively (n = 3, *P < 0.05, **P < 0.01, ***P < 0.001) (B) Western blot analysis of RPE-specific markers and mesenchymal markers in fRPE with or without EMT changes. The expression levels of RPE markers were downregulated and the expression levels of EMT markers were upregulated in EMT fRPE. (C-D) Immunocytochemistry results showed similar trends. (Blue: DAPI)

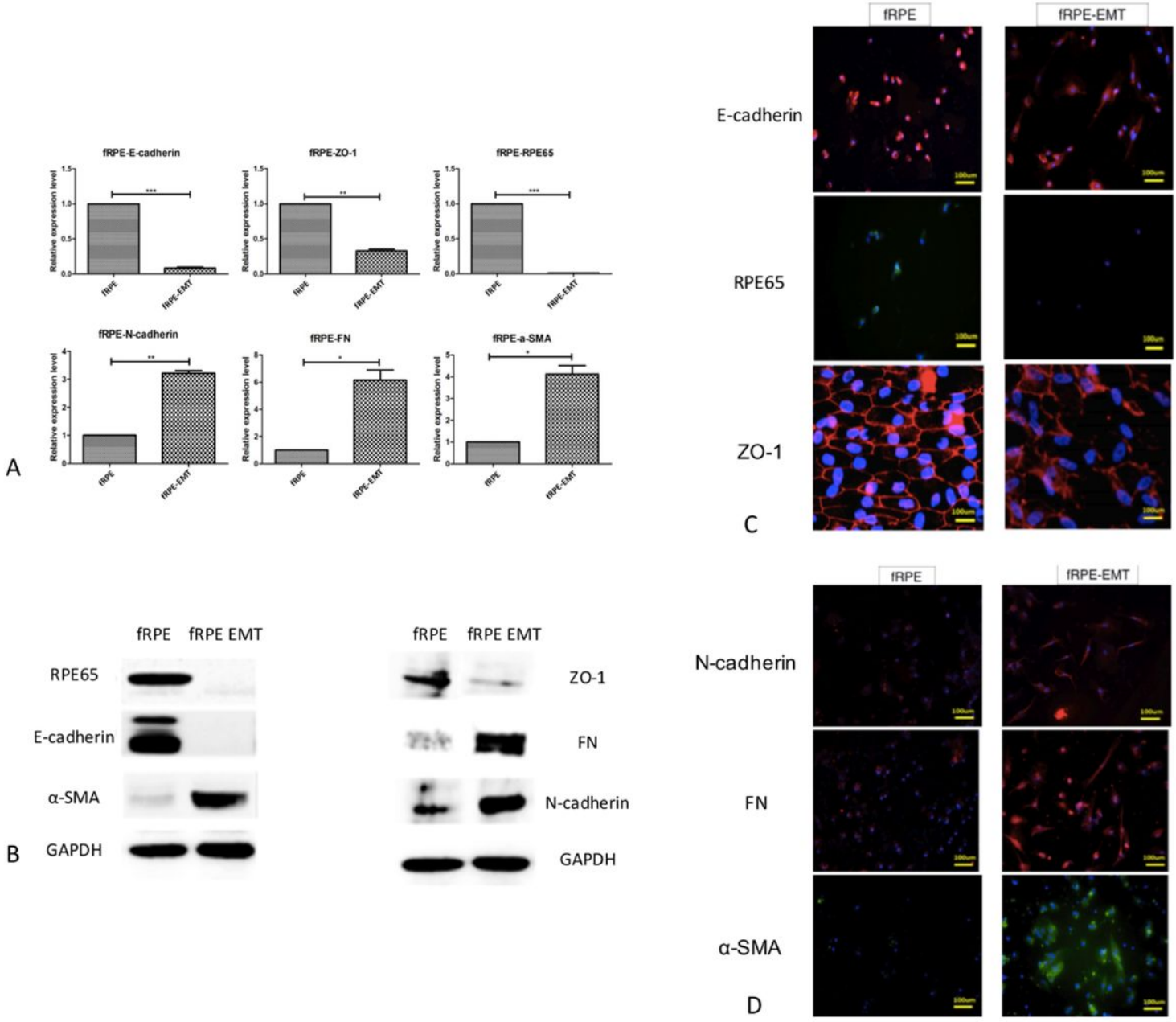

Figure 3

Expression of RPE-specific markers and mesenchymal markers EMT in fRPE.(A) RT–qPCR analysis of RPE-specific markers and mesenchymal markers in fRPE with or without EMT changes: It showed that RPE65, E-cadherin and ZO-1 expression in fRPE cells undergone EMT changes were significantly decreased and a-SMA, N-cadherin and FN were significantly increased by 4.12 folds, 3.21 folds and 10.26 folds respectively (n = 3, *P < 0.05, **P < 0.01, ***P < 0.001) (B) Western blot analysis of RPE-specific

markers and mesenchymal markers in fRPE with or without EMT changes. The expression levels of RPE markers were downregulated and the expression levels of EMT markers were upregulated in EMT fRPE. (C-D) Immunocytochemistry results showed similar trends. (Blue: DAPI)

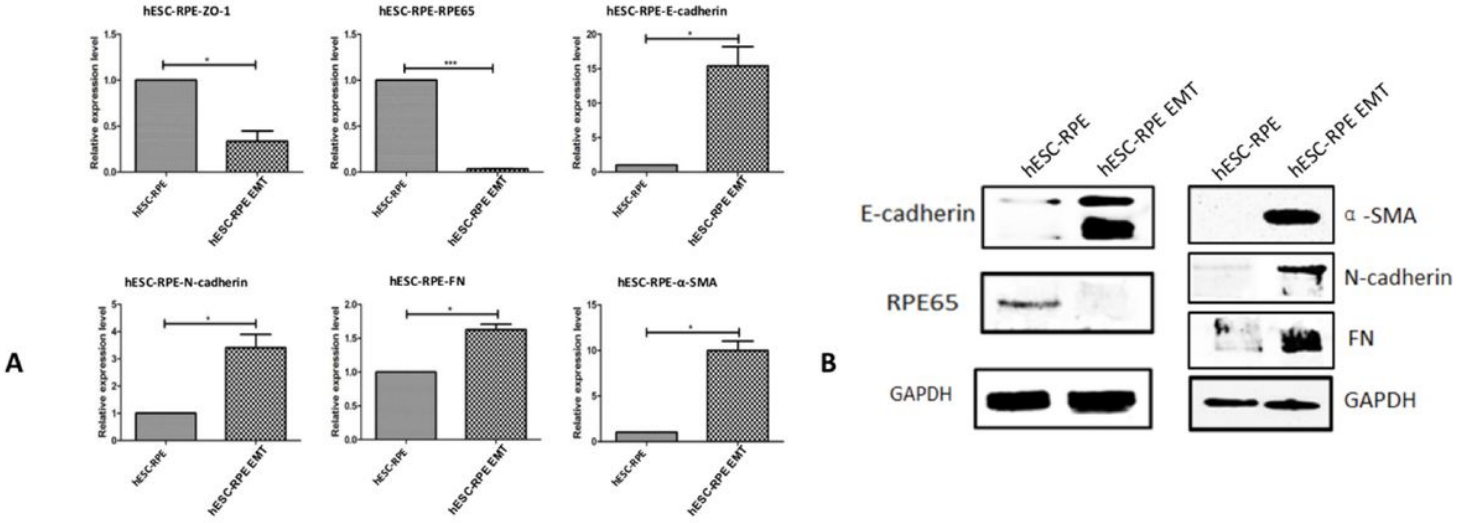

Figure 4

Expression of RPE-specific markers and mesenchymal markers EMT in hESC-RPE. (A) RT-PCR results showed that RPE65 and ZO-1 expression in hESC-RPE cells undergone EMT changes were significantly decreased and a-SMA, N-cadherin and FN expression were significantly increased. However, E-cadherin expression was upregulated in hESC-RPE, which was different from the trend of fRPE (n = 3, *P < 0.05, **P < 0.01, ***P < 0.001); (B) Western blot results demonstrated that protein expression levels of RPE markers were downregulated except E-cadherin, and the protein expression levels of EMT markers was found to be upregulated in mesenchymal hESC-RPE.

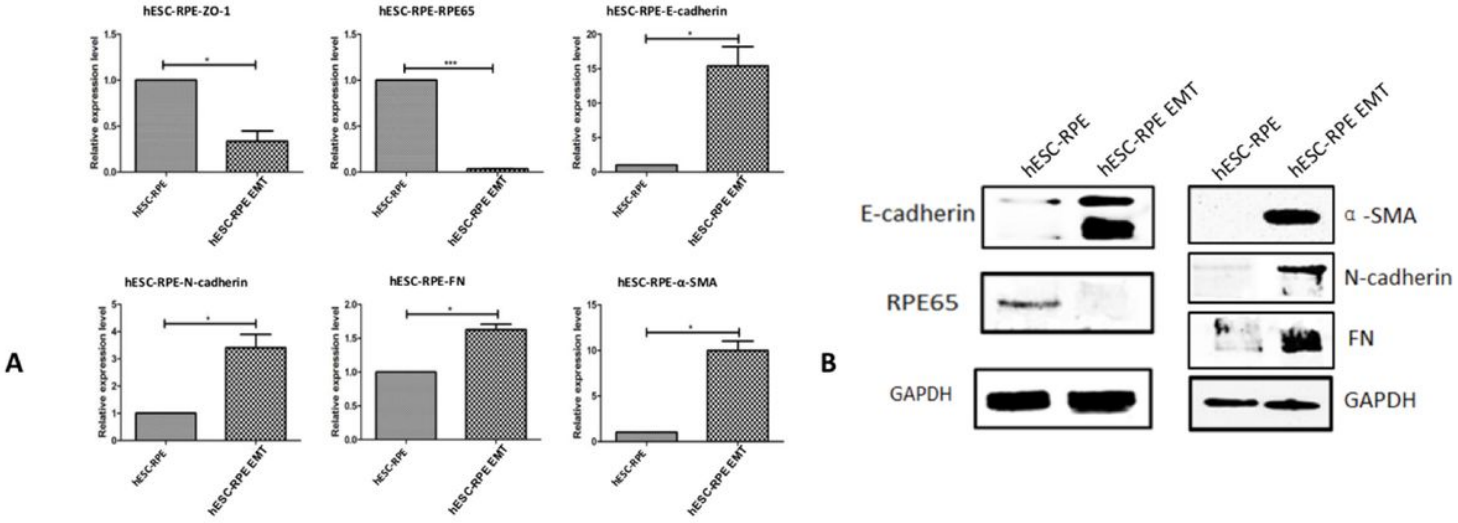

Figure 4

Expression of RPE-specific markers and mesenchymal markers EMT in hESC-RPE. (A) RT-PCR results showed that RPE65 and ZO-1 expression in hESC-RPE cells undergone EMT changes were significantly

decreased and a-SMA, N-cadherin and FN expression were significantly increased. However, E-cadherin expression was upregulated in hESC-RPE, which was different from the trend of fRPE (n = 3, *P < 0.05, **P < 0.01, ***P < 0.001); (B) Western blot results demonstrated that protein expression levels of RPE markers were downregulated except E-cadherin, and the protein expression levels of EMT markers was found to be upregulated in mesenchymal hESC-RPE.

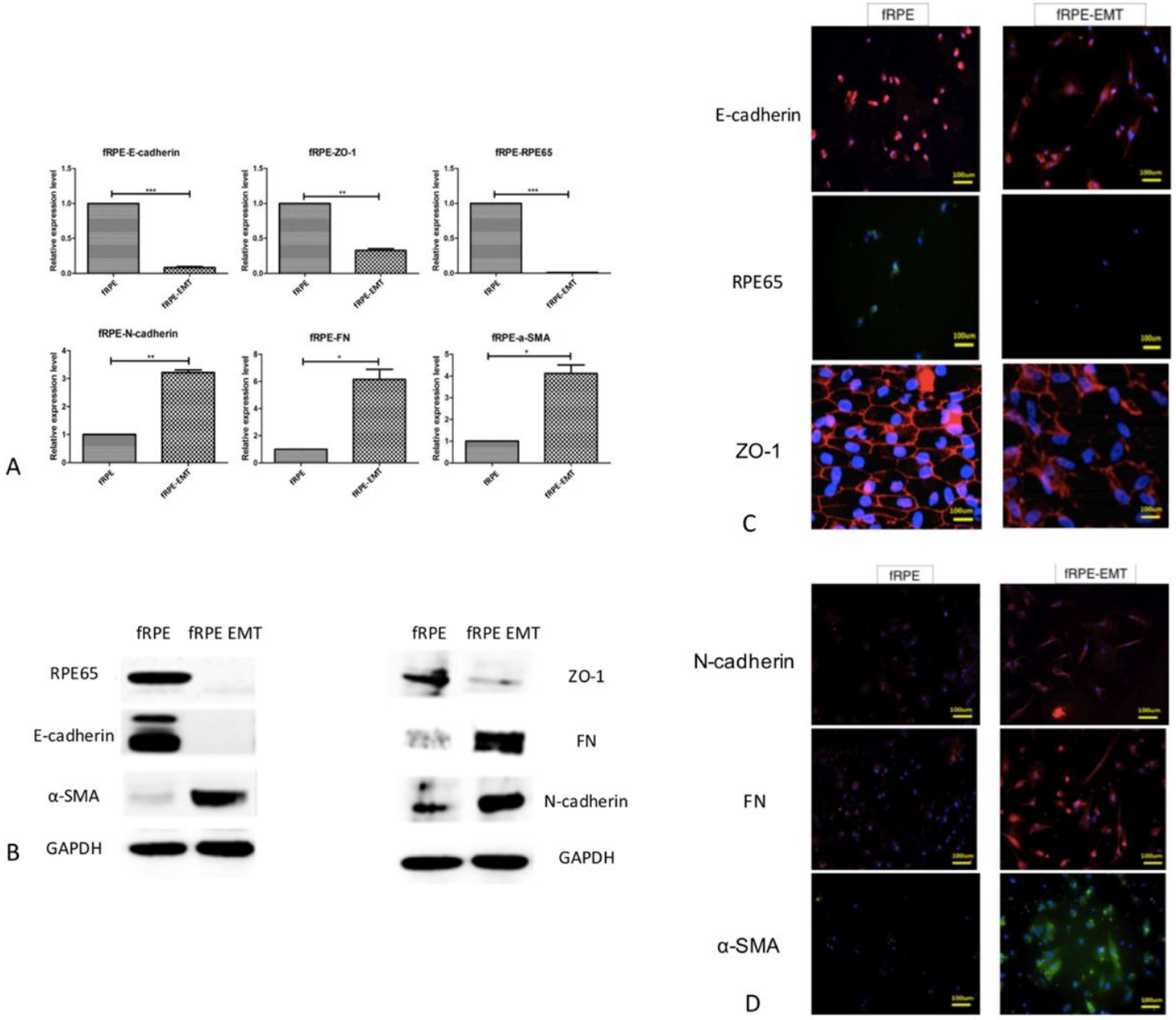

Figure 4

Expression of RPE-specific markers and mesenchymal markers EMT in fRPE.(A) RT–qPCR analysis of RPE-specific markers and mesenchymal markers in fRPE with or without EMT changes: It showed that RPE65, E-cadherin and ZO-1 expression in fRPE cells undergone EMT changes were significantly decreased and a-SMA, N-cadherin and FN were significantly increased by 4.12 folds, 3.21 folds and 10.26 folds respectively (n = 3, *P < 0.05, **P < 0.01, ***P < 0.001) (B) Western blot analysis of RPE-specific

markers and mesenchymal markers in fRPE with or without EMT changes. The expression levels of RPE markers were downregulated and the expression levels of EMT markers were upregulated in EMT fRPE. (C-D) Immunocytochemistry results showed similar trends. (Blue: DAPI)

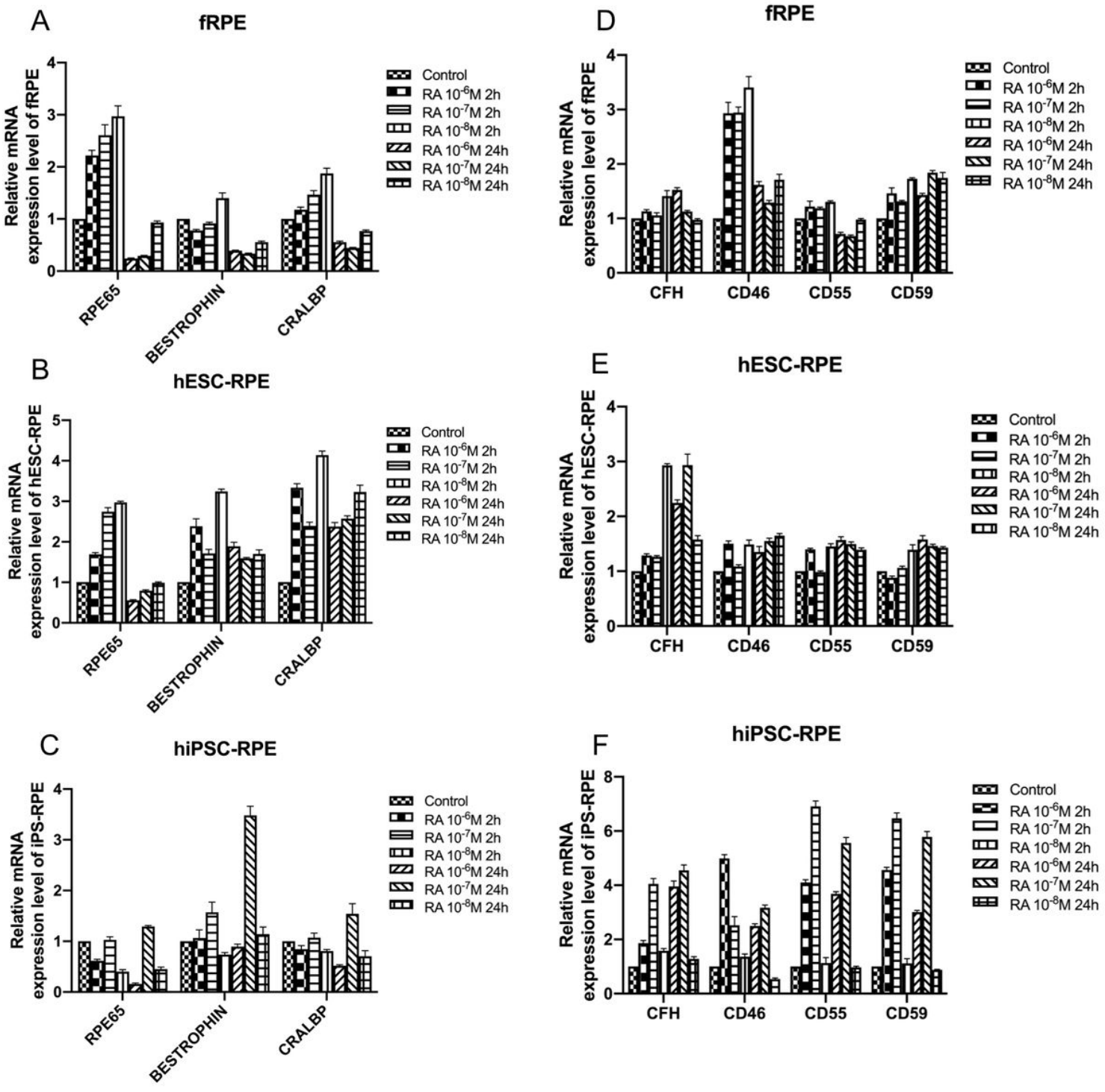

Figure 5

(A-C) Effect of ATRA on expression of RPE-specific gene in fRPE, hESC-RPE and hiPSC-RPE: (A)Incubation fRPE for 2 h with ATRA in different concentrations resulted in an increased expression of RPE65 and CRALBP genes. Incubation fRPE with ATRA in concentrations of 10-6 M and 10-7 M for 2 h did not

increase expression levels of Bestrophin gene. In contrast, after incubating with ATRA for 24 h, the mRNA expression levels of RPE65, BEST and CRALBP were decreased; (B) Incubation hESC-RPE for 2 h with ATRA in different concentrations resulted in increased gene expressions of RPE65, Bestrophin and CRALBP. However, 24-h RA incubation can sustainably upregulate Bestrophin and CRALBP gene expression; (C) RPE markers in hiPSC-RPE cells were upregulated by ATRA treatment in a concentration of 10-7 M either for 2 hours or 24 hours. (D-F) Effect of ATRA on expression of compliment negative associated gene in fRPE, hESC-RPE and hiPSC-RPE: In general, after 2-h or 24-h ATRA incubation, the expression levels of CRPs genes including CFE, CD46, CD55 and CD59 in all three RPE cell types were enhanced significantly.

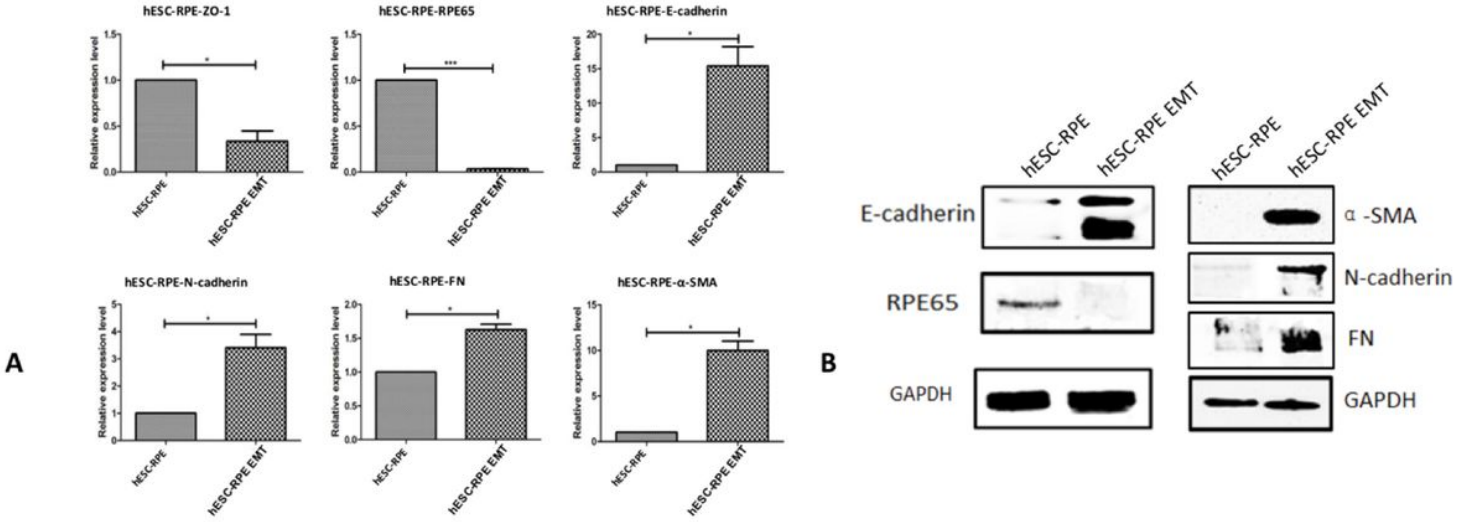

Figure 5

Expression of RPE-specific markers and mesenchymal markers EMT in hESC-RPE. (A) RT-PCR results showed that RPE65 and ZO-1 expression in hESC-RPE cells undergone EMT changes were significantly decreased and a-SMA, N-cadherin and FN expression were significantly increased. However, E-cadherin expression was upregulated in hESC-RPE, which was different from the trend of fRPE (n = 3, *P < 0.05, **P < 0.01, ***P < 0.001); (B) Western blot results demonstrated that protein expression levels of RPE markers were downregulated except E-cadherin, and the protein expression levels of EMT markers was found to be upregulated in mesenchymal hESC-RPE.

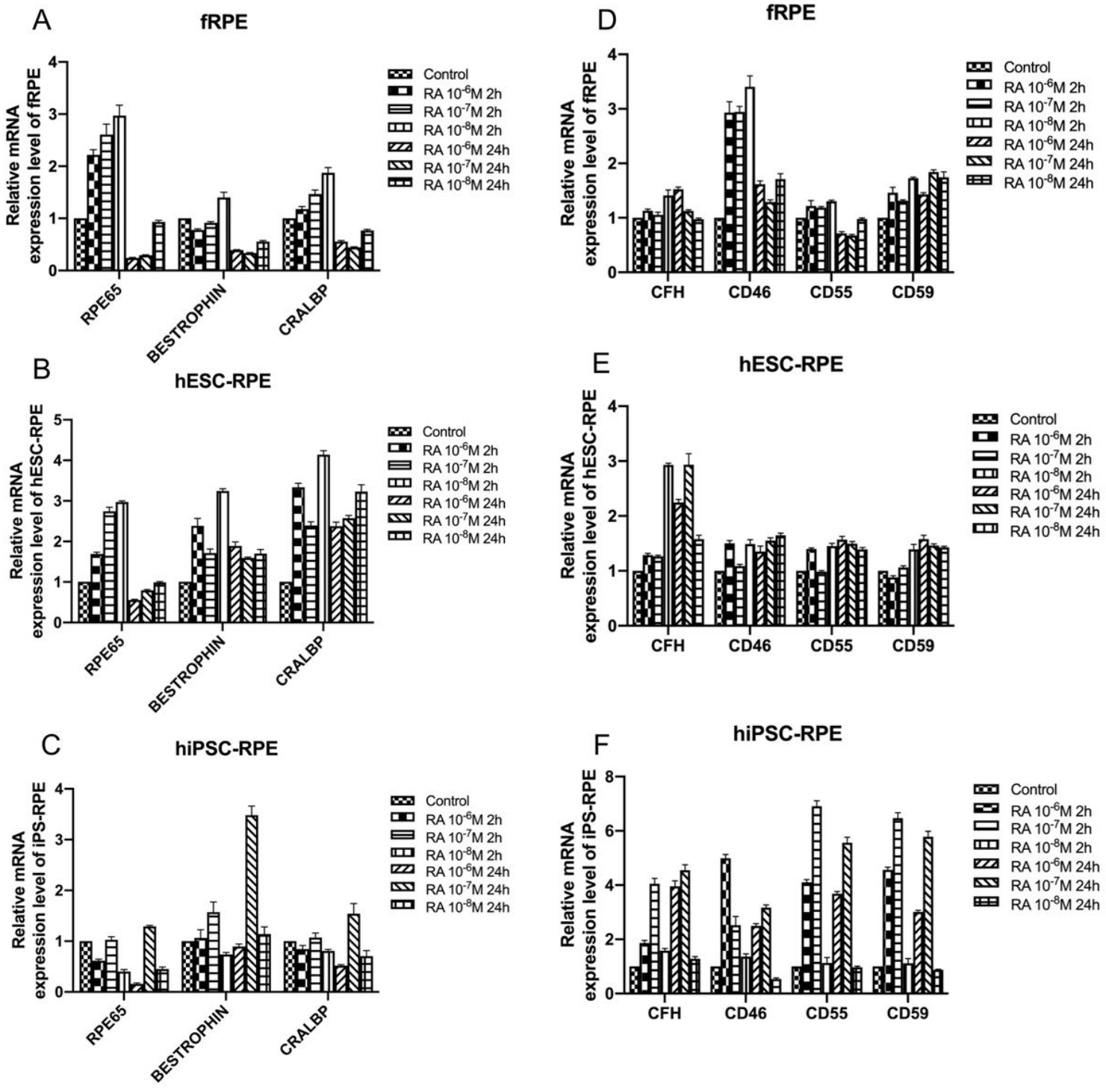

Figure 5

(A-C) Effect of ATRA on expression of RPE-specific gene in fRPE, hESC-RPE and hiPSC-RPE: (A)Incubation fRPE for 2 h with ATRA in different concentrations resulted in an increased expression of RPE65 and CRALBP genes. Incubation fRPE with ATRA in concentrations of 10-6 M and 10-7 M for 2 h did not increase expression levels of Bestrophin gene. In contrast, after incubating with ATRA for 24 h, the mRNA expression levels of RPE65, BEST and CRALBP were decreased; (B) Incubation hESC-RPE for 2 h with ATRA in different concentrations resulted in increased gene expressions of RPE65, Bestrophin and

CRALBP. However, 24-h RA incubation can sustainably upregulate Bestrophin and CRALBP gene expression; (C) RPE markers in hiPSC-RPE cells were upregulated by ATRA treatment in a concentration of 10-7 M either for 2 hours or 24 hours. (D-F) Effect of ATRA on expression of compliment negative associated gene in fRPE, hESC-RPE and hiPSC-RPE: In general, after 2-h or 24-h ATRA incubation, the expression levels of CRPs genes including CFE, CD46, CD55 and CD59 in all three RPE cell types were enhanced significantly.

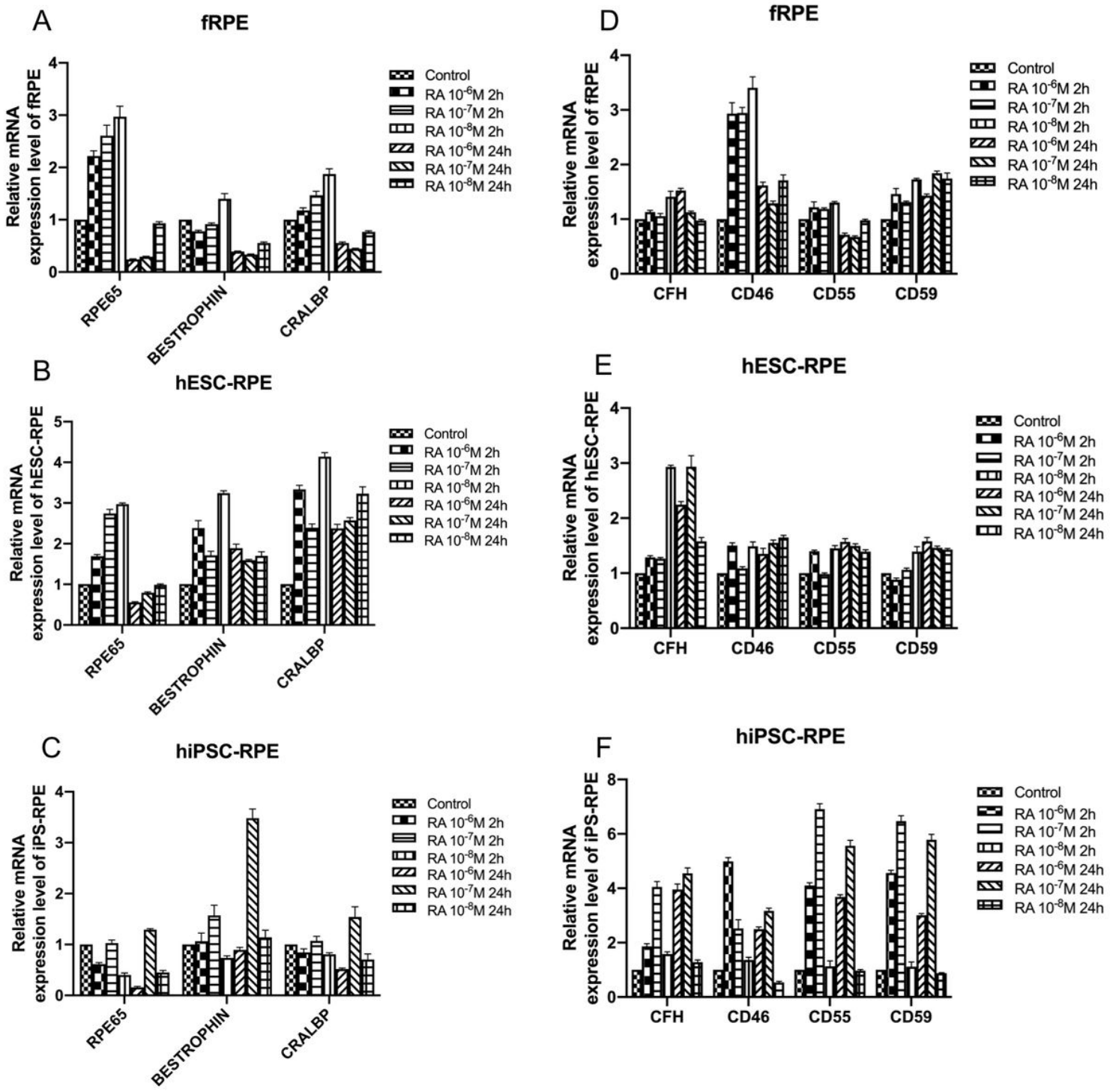

Figure 6

(A-C) Effect of ATRA on expression of RPE-specific gene in fRPE, hESC-RPE and hiPSC-RPE: (A)Incubation fRPE for 2 h with ATRA in different concentrations resulted in an increased expression of RPE65 and CRALBP genes. Incubation fRPE with ATRA in concentrations of 10-6 M and 10-7 M for 2 h did not increase expression levels of Bestrophin gene. In contrast, after incubating with ATRA for 24 h, the mRNA expression levels of RPE65, BEST and CRALBP were decreased; (B) Incubation hESC-RPE for 2 h with ATRA in different concentrations resulted in increased gene expressions of RPE65, Bestrophin and CRALBP. However, 24-h RA incubation can sustainably upregulate Bestrophin and CRALBP gene expression; (C) RPE markers in hiPSC-RPE cells were upregulated by ATRA treatment in a concentration of 10-7 M either for 2 hours or 24 hours. (D-F) Effect of ATRA on expression of compliment negative associated gene in fRPE, hESC-RPE and hiPSC-RPE: In general, after 2-h or 24-h ATRA incubation, the expression levels of CRPs genes including CFE, CD46, CD55 and CD59 in all three RPE cell types were enhanced significantly.

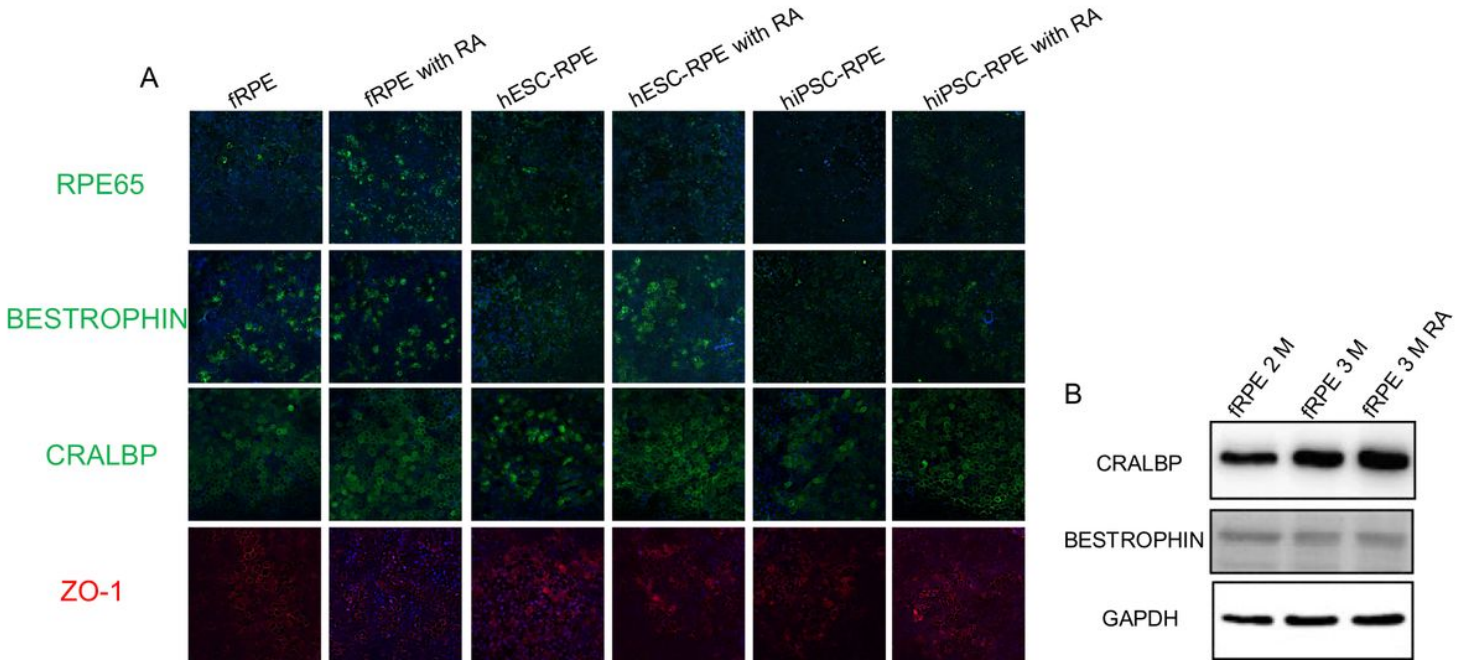

Figure 6

Expression of RPE-specific proteins in fRPE, hESC-RPE and hiPSC-RPE with or without RA treatment. (Blue: DAPI) (A) After incubating with 10-7 M RA for 2 h, the overall expression levels of RPE markers in three types of RPE cells increased. (B) Extended cultivating time and ATRA treatment increased expression levels of CRALBP protein in fRPE. However, no similar trends were shown in the expression level of Bestrophin protein in fRPE.

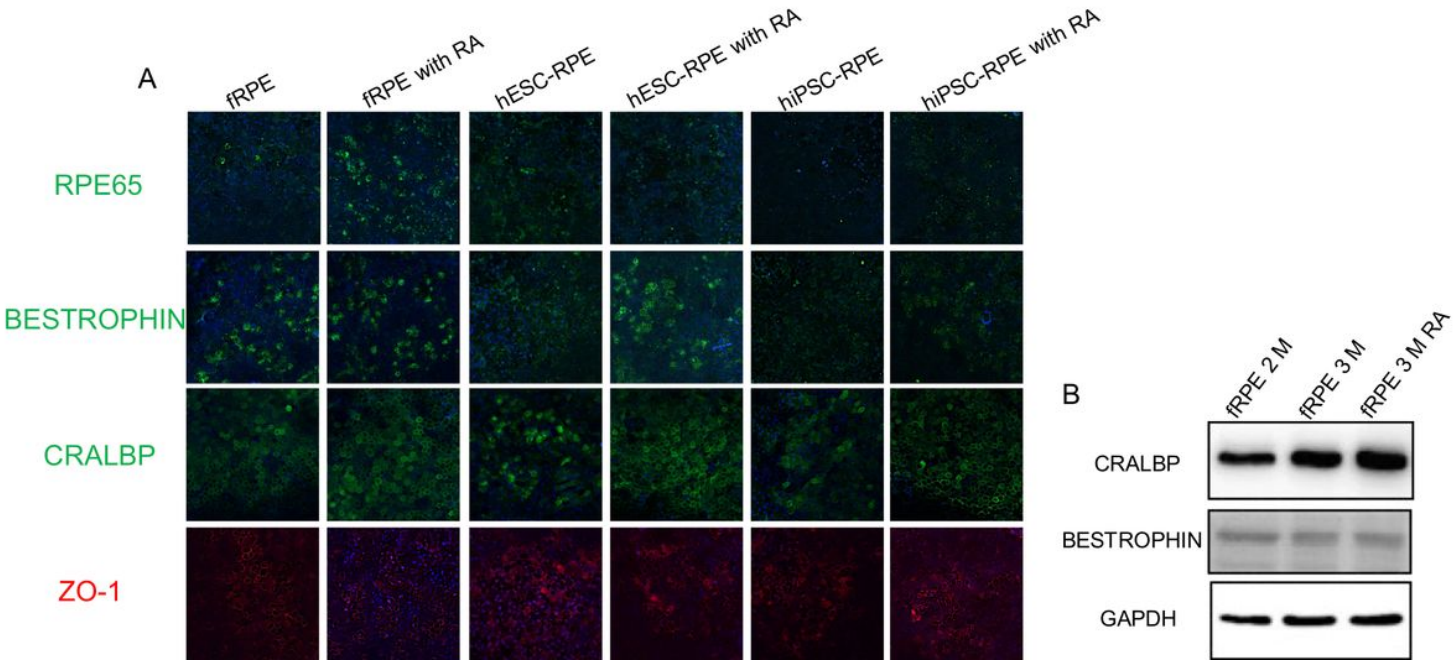

Figure 6

Expression of RPE-specific proteins in fRPE, hESC-RPE and hiPSC-RPE with or without RA treatment. (Blue: DAPI) (A) After incubating with 10-7 M RA for 2 h, the overall expression levels of RPE markers in three types of RPE cells increased. (B) Extended cultivating time and ATRA treatment increased expression levels of CRALBP protein in fRPE. However, no similar trends were shown in the expression level of Bestrophin protein in fRPE.

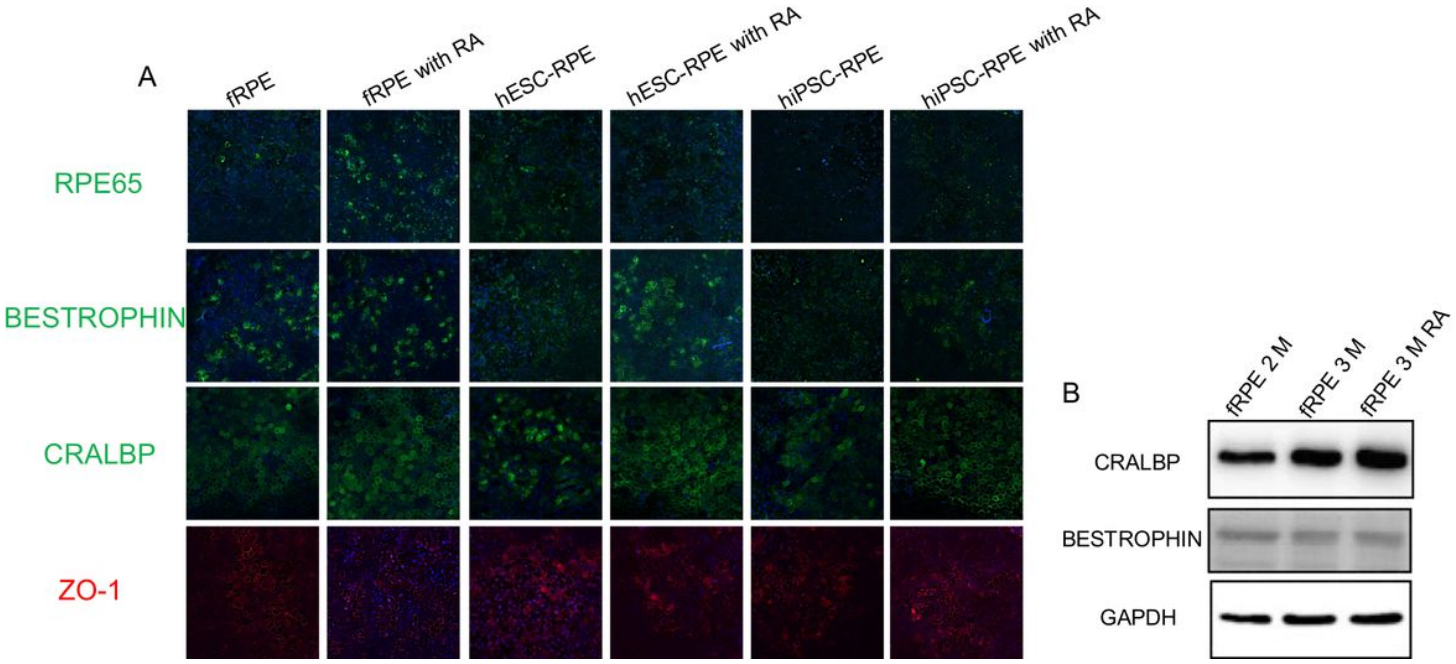

Figure 6

Expression of RPE-specific proteins in fRPE, hESC-RPE and hiPSC-RPE with or without RA treatment. (Blue: DAPI) (A) After incubating with 10-7 M RA for 2 h, the overall expression levels of RPE markers in three types of RPE cells increased. (B) Extended cultivating time and ATRA treatment increased expression levels of CRALBP protein in fRPE. However, no similar trends were shown in the expression level of Bestrophin protein in fRPE.

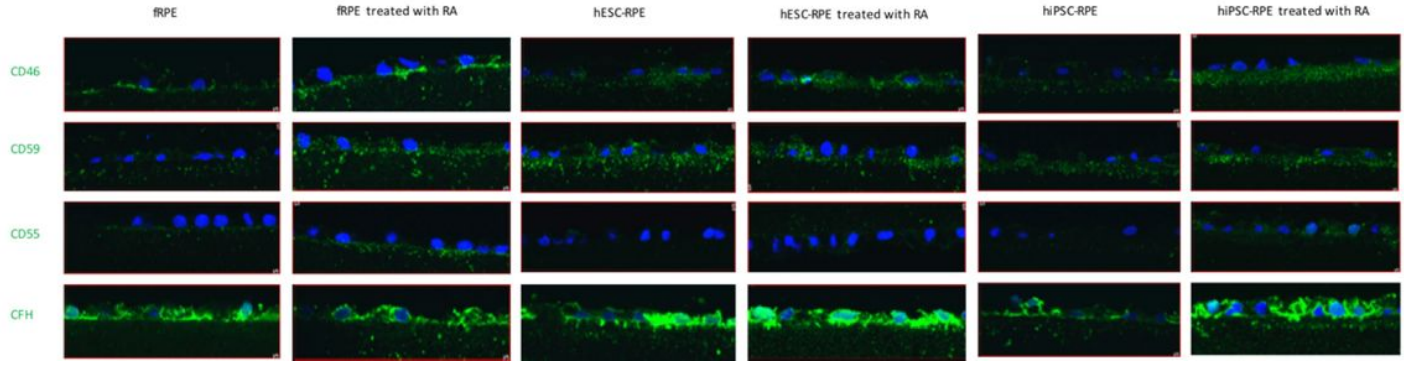

Figure 7

Expression of complement regulator proteins in RPE from different sources with or without RA treatment. There was a basal locating pattern of CD46 and CD55 protein expression in all three types of RPE cells. CFH and CD59 were secreted allover in cytoplasm in all three types of RPE cells. Incubation with 10-7 M RA for 2 h, the expression levels of CRPs protein in all three types of RPE cells were upregulated. (Blue: DAPI)

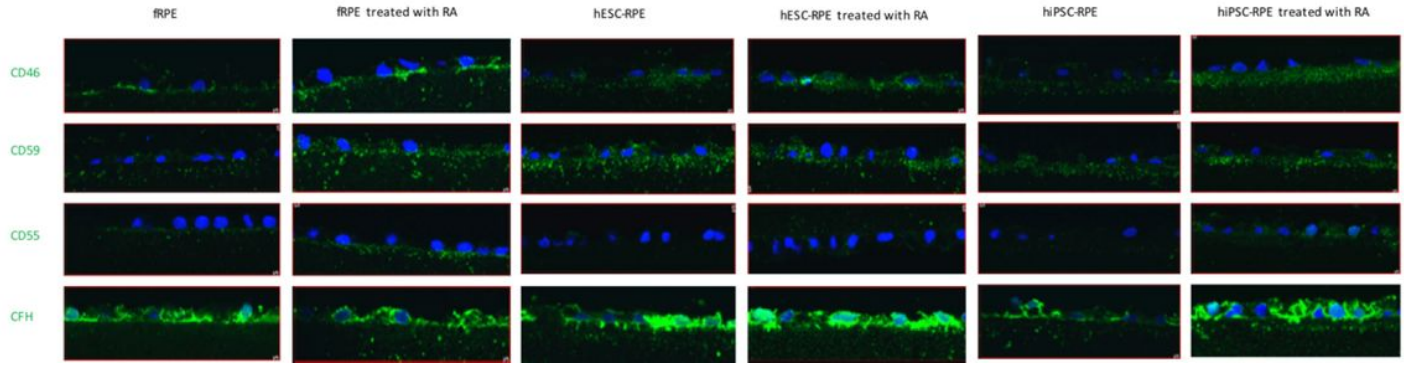

Figure 7

Expression of complement regulator proteins in RPE from different sources with or without RA treatment. There was a basal locating pattern of CD46 and CD55 protein expression in all three types of RPE cells. CFH and CD59 were secreted allover in cytoplasm in all three types of RPE cells. Incubation with 10-7 M RA for 2 h, the expression levels of CRPs protein in all three types of RPE cells were upregulated. (Blue: DAPI)

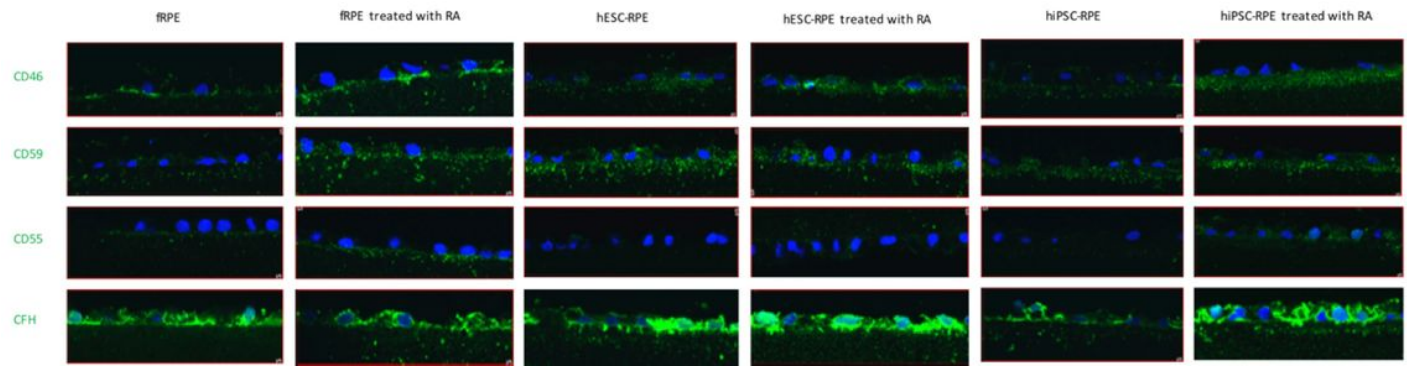

Figure 7

Expression of complement regulator proteins in RPE from different sources with or without RA treatment. There was a basal locating pattern of CD46 and CD55 protein expression in all three types of RPE cells. CFH and CD59 were secreted allover in cytoplasm in all three types of RPE cells. Incubation with 10-7 M RA for 2 h, the expression levels of CRPs protein in all three types of RPE cells were upregulated. (Blue: DAPI)

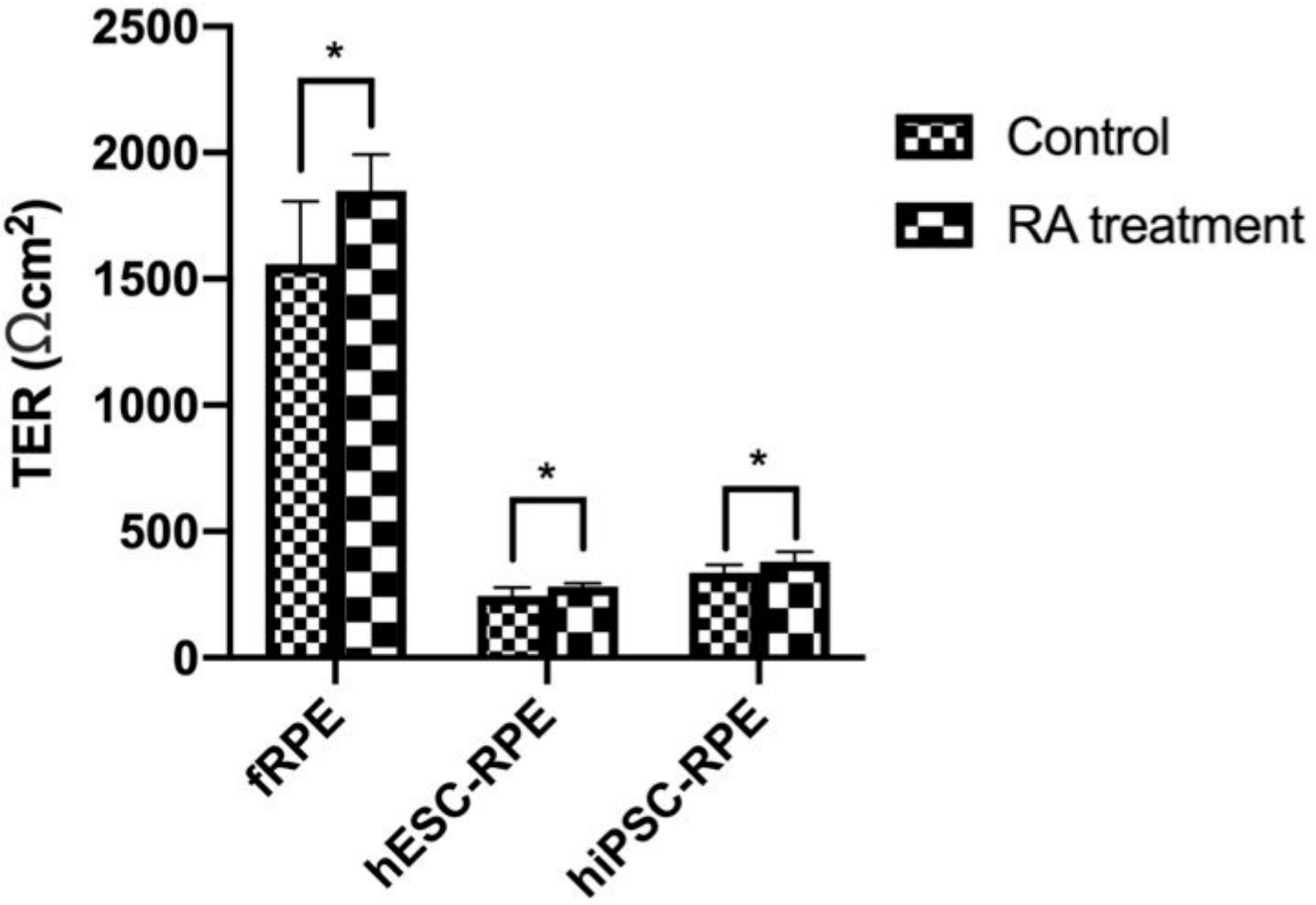

Figure 8

Barrier function changes in RPE from different sources with or without RA treatment. TERs were significantly increased in the RA incubation group. TERs of stem cell-derived RPE were significantly lower than those of fRPE and there were no significant differences in TERs between hESC-RPE and hiPSC-RPE. *P < 0.05, **P < 0.001.

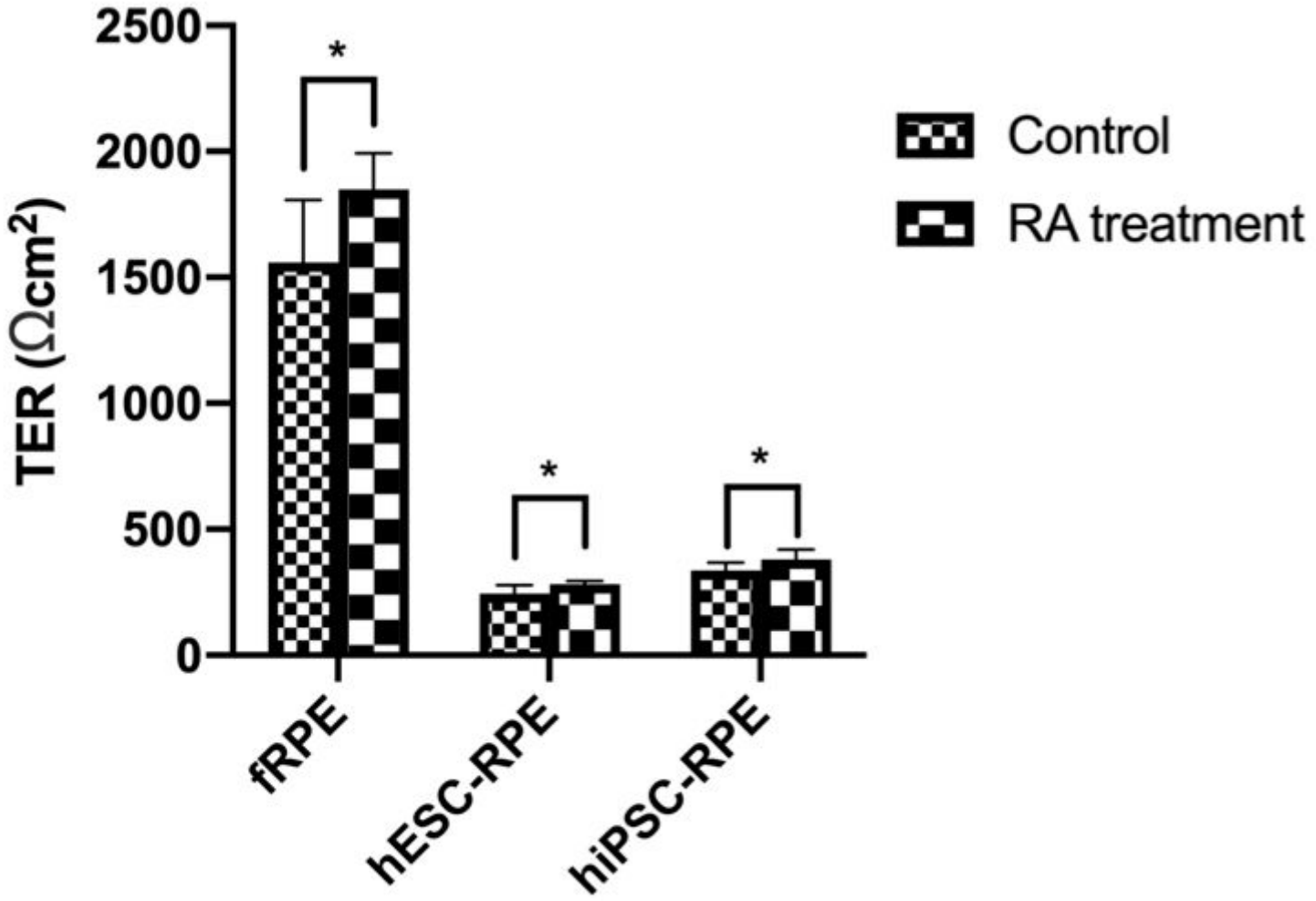

Figure 8

Barrier function changes in RPE from different sources with or without RA treatment. TERs were significantly increased in the RA incubation group. TERs of stem cell-derived RPE were significantly lower than those of fRPE and there were no significant differences in TERs between hESC-RPE and hiPSC-RPE. *P < 0.05, **P < 0.001.

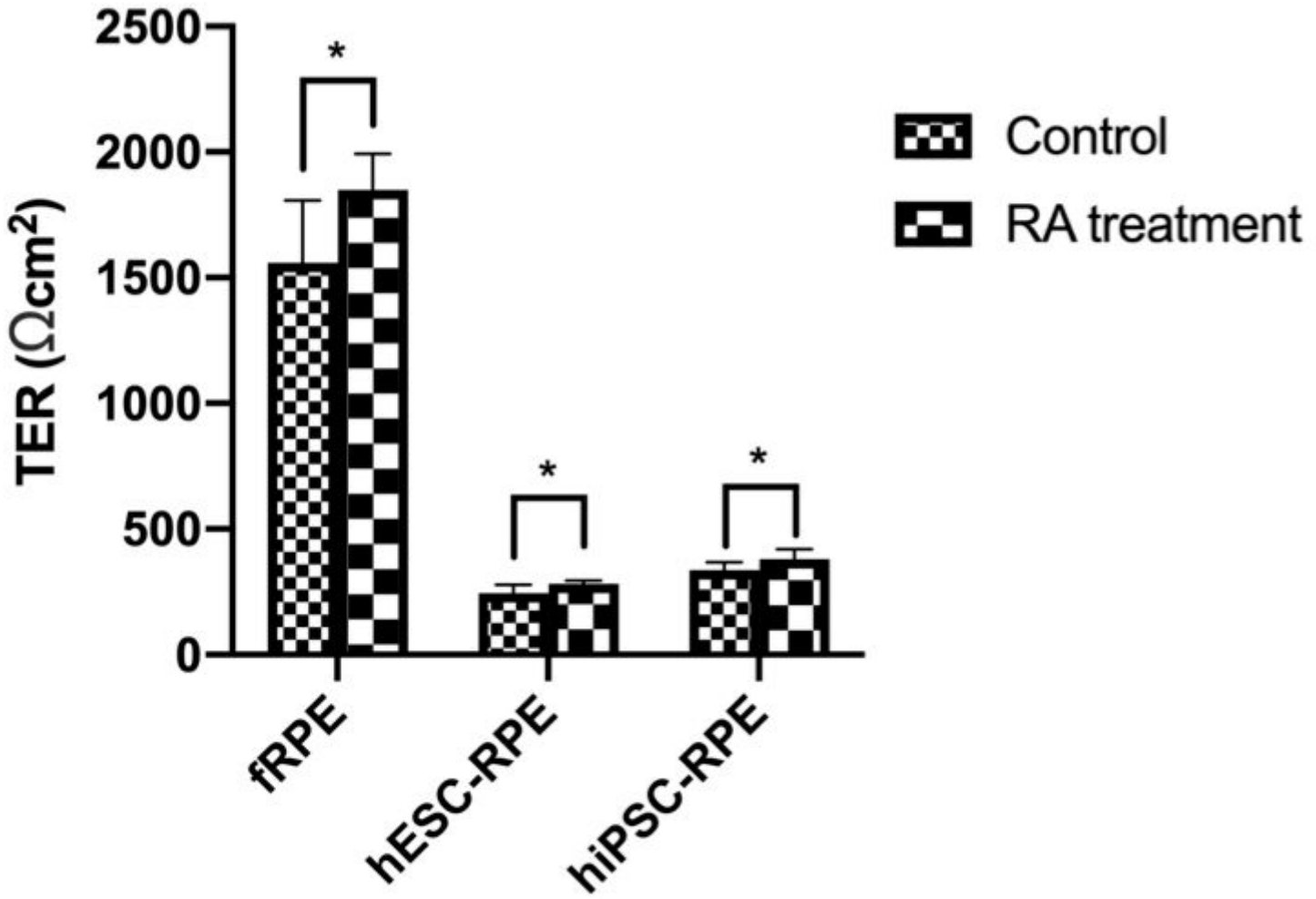

Figure 9

Barrier function changes in RPE from different sources with or without RA treatment. TERs were significantly increased in the RA incubation group. TERs of stem cell-derived RPE were significantly lower than those of fRPE and there were no significant differences in TERs between hESC-RPE and hiPSC-RPE. *P < 0.05, **P < 0.001.

Supplementary Files

This is a list of supplementary files associated with this preprint. Click to download.

- Additionalfile1TableS1.jpg
- Additionalfile1TableS1.jpg
- Additionalfile2FigS1.jpg
- Additionalfile3FigS2.jpg
- Additionalfile3FigS2.jpg
- Additionalfile3FigS2.jpg

- Additionalfile4FigS3.jpg
- Additionalfile4FigS3.jpg
- Additionalfile5FigS4.jpg
- Additionalfile5FigS4.jpg
- Additionalfile5FigS4.jpg
- Additionalfile6FigS5.jpg
- Additionalfile6FigS5.jpg
- Additionalfile6FigS5.jpg
- Supplementaryinformation.docx
- Supplementaryinformation.docx
- Supplementaryinformation.docx
- Additionalfile2FigS1.jpg
- Additionalfile2FigS1.jpg